The Luminosity Function of the Coma Cluster Core for

 $-25 < M_R < -11$

G. M. Bernstein¹

Dept. of Astronomy, 829 Dennison Bldg., University of Michigan, Ann Arbor, MI 48109 Electronic mail: garyb@astro.lsa.umich.edu

R. C. Nichol

Dept. of Astronomy and Astrophysics, University of Chicago, 5460 S. Ellis Ave., Chicago, IL 60637

Electronic mail: nichol@huron.uchicago.edu

J. A. Tyson¹

AT&T Bell Laboratories, Room 1D432, Murray Hill, NJ 07974 Electronic mail: tyson@physics.att.com

M. P. Ulmer¹

Dept. of Physics and Astronomy, Northwestern University, Evanston, IL 60208 Electronic mail: ulmer@ossenu.astro.nwu.edu

and

D. Wittman

Steward Observatory, University of Arizona, Tucson, AZ 85721 Electronic mail: dwittman@as.arizona.edu

ABSTRACT

We determine the luminosity function (LF) of galaxies in the core of the Coma cluster for $M_R \leq -11.4$ (assuming $H_0 = 75 \text{ km s}^{-1} \text{ Mpc}^{-1}$), a magnitude regime previously explored only in the Local Group. Objects are counted in a deep CCD image of Coma having RMS noise of 27.7 R mag arcsec⁻². A correction for objects in the foreground or background of the Coma cluster—and the uncertainty in this correction—are determined from images of five other

¹Visiting Astronomer, Kitt Peak National Observatory

high-latitude fields, carefully matched to the Coma image in both resolution and noise level. Accurate counts of Coma cluster members are obtained as faint as R = 25.5, or $M_R = -9.4$. The LF for galaxies is well fit by a power law $dN/dL \propto L^{\alpha}$, with $\alpha = -1.42 \pm 0.05$, over the range $-19.4 < M_R < -11.4$; faintward of this range, the galaxies are unresolved and indistinguishable from globular clusters, but the data are consistent with an extrapolation of the power law. Surface brightness biases are minimized since galaxies are not subjected to morphological selection, and the limiting detection isophote is 27.6 R mag arcsec⁻². We find the typical $M_R \approx -12$ Coma cluster galaxy to have an exponential scale length ≈ 200 pc, similar to Local Group galaxies of comparable magnitude. These extreme dwarf galaxies show a surface density increasing towards the giant elliptical NGC 4874 as $r^{-1.3}$, similar to the diffuse light and globular cluster distributions. The luminosity in the detected dwarf galaxies is at most a few percent of the total diffuse light of the giant galaxies in the cluster, and the contribution of the dwarfs to the mass of the cluster is likely negligible as well.

1. Introduction

In this paper we endeavor to determine the luminosity function (LF) of galaxies to the faintest limiting magnitudes accessible to modern telescopes. The LF is one of the cornerstone observations used in the study of galaxy formation. It also has fundamental importance for the empirical study and understanding of faint galaxy populations. For example, the Local Group is awash with dwarf spheroidal galaxies, nearly all of which appear to have formed the majority of their stars in discrete events. At faint apparent magnitudes we might be viewing ancestors of dwarf spheroidals undergoing star formation events, so it behooves us to measure the density of extreme dwarf galaxies in environments other than the Local Group.

To ease the task of identifying and counting the faintest possible galaxies, we look where we are likely to see the most galaxies: in the core of the Coma cluster. These measurements will further our understanding of the galaxy formation process by giving direct observations of an extreme case (low mass galaxies in dense environments). Luminosity functions of field galaxies can be derived from redshift surveys of apparent-magnitude-limited samples, but such surveys are dominated by distant giants and hence very inefficient at finding low-luminosity galaxies. The Stromlo-APM redshift survey of 1800 $b_J < 17.15$ galaxies

determines the galaxy luminosity function only for $M_{b_J} < -15$ (Loveday *et al.* 1992); the CfA redshift survey determines the LF for $M_{\rm Zw} \le -13$ (Marzke, Huchra, & Geller 1994); and a recent survey by Ellis *et al.* (1995) determines the LF for $M_{b_J} < -15$. These surveys all find that the faint end of the LF follows a power law $dN/dL \propto L^{\alpha}$ with $\alpha \approx -1.0$.

An alternative route to the galaxy LF, which we choose, is to identify all members of a galaxy cluster, and assume that all the identified galaxies are at a common cluster distance. The cluster method has the advantage that it does not require spectroscopy to obtain a redshift for every galaxy, and therefore cluster galaxy LFs are known to fainter magnitudes than the field LF. The obvious disadvantage to using clusters to determine the galaxy LF is that one measures the LF of the cluster, not of the Universe as a whole. Nonetheless the LF of clusters are interesting in their own right, since differences between cluster LFs can be direct evidence for environmental effects on galaxy formation. In contrast, if a universal LF is derived for all clusters it provides important insights into the underlying physics of cluster formation.

The benchmark in the study of cluster LFs is provided by Sandage et al. (1985, SBT85) with their measurement of the Virgo cluster for $M_B < -12$. They derive a faint-end slope of $\alpha \approx -1.35$ which is strikingly different from the value in the field. In addition to this work, Bothun et al. (1991) survey both Virgo and Fornax for LSB galaxies using photographic amplification, with a limiting surface brightness of 27 B mag arcsec⁻², and found many galaxies missed by SBT85. This demonstrates the importance of surface-brightness selection effects in such magnitude-limited galaxy catalogs, as emphasized by Disney (1973). In contrast, CCDs reach lower surface brightness thresholds as demonstrated by Turner et al. (1993, and references therein) who surveyed sections of A3574 to a limiting isophote of 26.7 V mag arcsec⁻². These subsequent studies have in general agreed with the original findings of SBT85, in that the faint end of the cluster LF follows a steeper power law than the field.

All the above studies, however, lack coverage of the field to comparable depth as the cluster, thus giving them no rigorous means of deciding which objects are in the cluster and which may be foreground/background contamination. Membership is decided primarily on morphological grounds, which leads to a bias against galaxies which are compact enough to resemble stars, or might be mistaken for background galaxies; conversely, background galaxies could be mistaken for cluster members.

We have conducted a measurement of the luminosity function of Coma cluster galaxies which is relatively free of morphological or surface-brightness bias, because rather than select cluster members individually by morphological criteria, we merely count the number of objects in an image of the Coma cluster core. The density of foreground and background

objects is determined by counting galaxies in images of 5 random high latitude control fields. Simple subtraction of the control counts from the counts in the Coma image yields a count of excess objects, which can be assumed to be members of the Coma cluster at redshift 7000 km s⁻¹. Because all Coma and control images are deep CCD exposures, our magnitude and surface-brightness thresholds are lower than in previous investigations: when optimally filtered for objects of size 1.3", the 3σ noise level in our images is 27.8 R mag arcsec⁻². The linear and digital nature of the CCD images also makes it possible to very closely match the characteristics of the Coma and control-field images, minimizing the problem of differential completeness which might otherwise cause error in the subtraction of foreground/background counts from the Coma counts. By having 5 distinct control fields, we may also determine the field-to-field variance on foreground/background counts, and thus can obtain error estimates on the net Coma cluster object counts in a model-independent manner. Only when there is some unique aspect to the Coma field relative to the control fields need we be concerned about possible systematic biases in our estimated Coma cluster LF.

Use of the more distant Coma cluster rather than Virgo actually makes the measurement easier. If we wish to observe galaxies of a given absolute magnitude M and a certain space density in the center of a cluster, the projected density of the galaxies on the sky will scale as $10^{0.4(M+\mu)}$, where μ is the distance modulus to the cluster under study. The surface density of superposed background galaxies in R band scales almostly exactly as $10^{0.4(M+\mu)}$ as well (Tyson 1988), so that the mean ratio of target objects to background objects is roughly independent of μ . The angular correlations of fainter background galaxies, are smaller, however, so the *fluctuations* in background counts are reduced for the more distant cluster. This gives better accuracy on the LF. As long as the objects are resolved, we pay no integration time penalty for the more distant cluster because the time required to image the galaxy at a given S/N increases as the square of the distance, but the solid angle subtended by the cluster (and hence the number of separate telescope pointings required) decreases as the square of the distance. What is sacrificed in a more distant survey is resolution of the target galaxies. Indeed in our survey we do not obtain morphological information on most of our dwarfs. Furthermore the faint-end limit to our LF arises not because of S/N considerations, but because we are unable to distinguish dwarf galaxies from globular clusters. The resolution and sensitivity of our images is such that most of the dwarf spheroidal galaxies known in the Local Group would be detected if they were at the distance of the Coma cluster, and our LF thus includes the first complete measure of the abundance of galaxies this faint. At $R \approx 23$ ($M_R \approx -12$) the brightest globular clusters in Coma are detected. Harris (1987) and Thompson & Valdes (1987, TV87) both detect globular clusters (and dwarf galaxies) around NGC 4874 in Coma, though in much

smaller fields than ours. Our ability to discern dwarfs from globular clusters disappears for $M_R > -11.4$.

We discuss in the next section the observations of the Coma and control fields, and the production of flattened images and object catalogs for these fields. The image processing steps are discussed in unusual detail, because the success of our method depends critically on the elimination of any systematic differences in detection efficiencies between the Coma field and the control fields; the trusting reader can skip these details. In §3 we present the methodology for deriving counts of Coma cluster members from the catalogs of Coma and control field images. We also enumerate several possible pitfalls in the application of this methodology to our data, concluding that none of them are of serious concern. In §4 the methodology is applied to derive the luminosity and size distributions of the members of the Coma cluster core, and the variation of their surface density with distance from the cluster center. In §5 we look in closer detail at the LF of galaxies in the Coma cluster, comparing our results to those of other clusters by other authors. We also estimate the masses required of these objects for tidal integrity. In §6 we discuss several possible evolutionary scenarios for the dwarf galaxies in Coma, and their relation to dwarfs in the field, and we give a brief summary and suggestions for future observations in §7. An extensive review of the properties of dwarf elliptical (dE) galaxies and their evolution is given by Ferguson & Binggeli (1994, FB94). Because the breadth of knowledge and speculation on dwarf galaxies is so large, we refer the interested reader to this review and minimize our rehashing of the literature. Though we have little direct knowledge of the morphology of the $M_R \sim -12$ galaxies in the Coma cluster, observations of nearer clusters detect few dwarf irregular galaxies, and these gas-rich galaxies are unlikely to be present in the core of Coma. We will therefore, for simplicity, often refer to the dwarfs in Coma as dE galaxies. We will assume a Hubble parameter of $H_0 = 75 \text{ km s}^{-1} \text{ Mpc}^{-1}$, giving a distance modulus of 34.9 for the Coma cluster. Under this assumption, 1" subtends 460 pc at the Coma cluster, and our field spans a 200 kpc square.

2. Creating the Object Catalogs

2.1. Observations

The Coma field was observed on 10 February 1991 from the KPNO 4-meter telescope, using a backside-illuminated 1024×1024 Tektronix CCD at prime focus. One pixel spans 0.473'' on the sky, giving an 8' field of view. A series of 27×300 second exposures was

taken in a "shift and stare" mode (Tyson 1986): the telescope pointing is different for each exposure, as much as 1′ from the nominal field center. After de-biasing and flat-fielding (discussed below), the relative offsets of the exposures are determined to ~ 0.1 pixel by photometry of bright stars, and the images are registered using bilinear interpolation. Note that the interpolation introduces correlations between adjacent pixels, so that the noise spectra of our images are not white. At each pixel, the signals from all 27 exposures are averaged, after a 3σ clip to remove cosmic ray events. The shifting reduces the high-S/N area of the final image to a 7.5′ square. The FWHM of the PSF in the final R-band image is 1.3″. This image is shown in Figure 1. The field is centered at approximately $12^{\rm h}57^{\rm m}30^{\rm s}$, $+28^{\circ}09'30''$ (1950), near the x-ray centroid of the cluster (Ulmer, Wirth, & Kowalski 1992). The giant elliptical galaxies NGC 4874 and NGC 4889 lie 40″ and 280″ off the NW and NE corners, respectively, of our frame. Exposures in the B_j filter were also obtained, but the seeing was too poor for these data to be useful for investigating the faintest Coma cluster galaxies.

The flat field for this run is produced in a two-step process: the small-scale structure is determined from dome flats. The large scale structure of the flat is determined from the median of 44 disregistered 300 second exposures of 7 distinct high-latitude fields which are free of large objects. These exposures were all taken during the same run as the Coma images, and are distinct from the high-latitude data used to determine background counts. This median blank-sky flat is then divided by the dome flat and smoothed, and the resulting image is multiplied by the dome flat to give the final flat-field image. When "blank-sky" exposures are processed using this flat-field, the remaining variations in the sky level are much smaller than the observed diffuse-light gradients in the Coma field, so we conclude that the measured diffuse signal is not significantly affected by flat-fielding errors.

Five regions of the sky were observed under nearly identical conditions for use as control fields in this study. These fields are selected at random, subject to the constraints that they have low extinction in the Burstein & Heiles (1982) map, and be free of bright $(R \leq 14)$ stars or galaxies. The characteristics of these control fields are listed in Table 1. Although these control exposures were not taken during the same run as the Coma image, they are all in the same filter band, all are taken at prime focus of either the KPNO or CTIO 4-meter telescopes, and all using thinned Tek1024 CCDs. The observing, flat-fielding, and image-combining techniques are the same as for the Coma field.

All of the fields were observed through the Kitt Peak Harris R filter, or the CTIO version of same. Two of the control fields contain faint standard stars from Tyson & Seitzer (1988, TS88); for the remainder, photometric zeropoints were transferred from observations of a TS88 field on the same night. The TS88 R band is for these purposes identical to the

Cousins R system. The Coma observations of February 1991 were non-photometric, with up to 0.7 mag of obscuration by clouds. The Coma field and a TS88 standard field were re-observed with the same setup on the photometric night of 14 June 1991 to determine the photometric zeropoint of the deep Coma image. We estimate the zeropoint accuracy of the fields to be 0.05 mag or better, based on variance of standards and a few repeat measurements.

2.2. Matching of Control Fields

The success of our differential counting method depends upon matching the detection characteristics of the control fields as closely as possible to those of the Coma field. Most of the control field images have better seeing and/or lower noise than the Coma image, so we degrade them to better match Coma. We first degrade the seeing of a control image by convolving it with a Gaussian of proper width to bring the FWHM of the PSF near the Coma FWHM of 2.77 pixels. The FWHM of the processed control fields, listed in Table 1, range from 2.71 to 2.81 pixels. Smoothing the control images in this way removes high-frequency noise—we therefore next add high-pass-filtered noise back into the images in order to restore the original noise power spectrum.

Three of the control images have lower noise than Coma, so we add noise to these images. The RMS sky signal fluctuations in the Coma image are 29.32 mag per pixel (surface brightness 27.7 mag arcsec⁻²); the control fields have noise levels from 29.19 to 29.37 mag per pixel. The noise power spectra, not just the RMS levels, are matched. In Table 1 we list the noise spectral densities of the Coma and matched control-field images. These numbers give the amplitude of the flat part of the noise power spectrum in our images; recall that some short-wavelength noise is removed by the bilinear interpolation during image registration. To estimate the RMS noise when the images are smoothed by a rectangular window of area A, multiply by $1/\sqrt{A}$; if the smoothing window is a Gaussian with dispersion σ , multiply by $1/\sqrt{\pi\sigma^2}$. It is important to specify the resolution or window size when quantifying a surface-brightness noise.

The control fields are thus very similar to the Coma field in resolution and noise, and hence in detection efficiency. We conduct Monte Carlo completeness measurements as described below to quantify the small remaining differences in detection efficiency among the fields. When reading the following sections, keep in mind that in §4.5. we detect a very strong gradient of Coma cluster members toward NGC 4874. If our signals were merely

errors in magnitude scale, extinction corrections, or completeness corrections, we would not expect to find such a gradient.

2.3. Removal of Diffuse Light

We cannot search for faint objects using the image shown in Figure 1 because the diffuse light gradient overwhelms the detection algorithms. We must remove the large-scale gradients from the Coma image in order to successfully use the FOCAS programs. We describe here the procedure used for this; because this procedure was not executed for the control fields, we must also be sure that it does not alter the signals from small objects in the Coma field, lest the subtraction of control counts be invalidated. The first step in the removal of the large-scale features of the image is to fit elliptical isophotes to the 23 brightest galaxies (and one bright star). The fitted ellipses are then subtracted from the image, allowing FOCAS to successfully search for dwarf galaxies where it previously was "blinded" by flux gradients due to giant galaxies. Regions where the elliptical isophotes are a poor fit are masked and ignored in further processing. Once these larger objects are subtracted, we fit the large-scale gradients in the image by running a 15"-square median filter across the image. These steps of galaxy fitting and diffuse-light subtraction must be iterated for best results, particularly in the NW corner of the image, which contains steep diffuse-light gradients from NGC 4874, another bright S0 galaxy, and a bright star.

The final step in the removal of the diffuse light is to use the FOCAS program DETECT to create a diffuse-light map of the field, and then subtract away this diffuse component. FOCAS tracks the sky level during its detection phase using an exponential average with a scale length of $\approx 40''$. This subtraction of the FOCAS "sky" image is done for the control fields as well as for the Coma field. The resulting cleaned and masked Coma image is shown in Figure 2, and the many low-luminosity objects are now clearly visible.

In Figure 1 it appears that the diffuse light gradient from NGC 4874 extends all the way across our image (see also the diffuse light plot in Figure 8). Is this diffuse light really present in the Coma cluster, or are we merely seeing scattered light from the core of NGC 4874 ($R \approx 11$) or the $m_V \approx 7$ stars SAO 082595 and SAO 082589 located within 30'? The tabulation of the distant wings of the typical seeing disk by King (1971) suggests that the scattered light should be much weaker than the observed diffuse light. This is verified by our own tests with the CTIO 4m prime focus camera, in which we image "blank" high-latitude fields within 1° of bright stars and search for diffuse scattered light. Since the

CTIO and KPNO 4m telescopes are very similar, we conclude that our diffuse-light signal originates in the Coma cluster, and is not an artifact of atmospheric or telescope optics.

2.4. Catalogs

The FOCAS software package (Valdes 1989) is used to detect and analyze objects in the six fields. For the uninitiated, the properties of FOCAS of relevance to this work are as follows: all objects are found which exceed local sky by more than 3σ (27.6 R mag arcsec⁻² in our images) in a filtered version of the image. On the unfiltered images these objects are checked for multiple maxima by an object-splitting algorithm. Several photometric quantities are calculated for each object using the unfiltered image. The two we use here are the "total" magnitude m_t , and the "core" magnitude m_c . The former is derived by growing the object several pixels in all directions around the original detection isophote and measuring the flux above sky inside this expanded region. This quantity m_t is shown by Monte Carlo tests to be an unbiased estimator of the true magnitude of unresolved objects. Our tests show that it remains unbiased for Gaussian-profile objects of any size, but does underestimate total magnitude for exponential-profile objects which are near the detection limit and have scale sizes large compared to the seeing disk (we will return to this question in $\S4.4$.). The core magnitude is the highest flux found in any contiguous 3×3 pixel subarea of the image, and thus is roughly the peak surface brightness. We will use $\mathcal{R} \equiv m_t - m_c$ as our resolution parameter, since unresolved objects have a nearly fixed value of \mathcal{R} . We prefer \mathcal{R} to the FOCAS "scale" parameter because the former takes continuous values and is more robust in crowded areas.

FOCAS is run with the same parameters for all six fields, except that the detection threshold is maintained at fixed increment above the (slightly varying) noise level. The detection threshold is chosen so that the number of false positive detections is negligible—Monte Carlo tests suggest that there are ~ 15 detections of noise with 25 < R < 25.5, and none with R < 25.

The final step in producing object lists is to delete from the catalogs those objects centered within 5" of any edge or masked area of the image. The useful area A_i of each field, excluding the masked areas and 5" buffer zones, is listed in Table 1.

2.5. Exclusion of Bright Foreground Stars

In Figure 3 we plot the R magnitude (the m_t values produced by FOCAS) versus the resolution parameter \mathcal{R} for all of the valid objects in the Coma field. At bright magnitudes the stellar locus at constant $\mathcal{R} \approx 0.65$ is apparent. For R < 21 we may confidently identify objects with $\mathcal{R} < 0.8$ as stellar; at fainter magnitudes the galaxy population begins to merge into the stellar locus, so we do not attempt object-by-object classification. The R-vs- \mathcal{R} plot for the 5 control fields are similar, and we identify as stellar those objects with R < 21 and $\mathcal{R} < 0.8$.

2.6. Extinction Correction

Counts of extragalactic background objects will be depressed by Galactic dust extinction, so we must compensate for this extinction if we are to use the control fields as models for the Coma background counts. We use the maps of Burstein & Heiles (1982) to determine the extinction in each field relative to that of Coma, assuming an R-band extinction $A_R = 2.5E_{B-V}$. A_R is only 0.03 mag in the Coma field itself. The detected R magnitudes of all objects in each control fields are adjusted brightward by the relative extinction corrections listed in Table 1. These corrections bring the control fields into agreement with the Coma extinction, not to zero extinction. The correction of 0.12 mag in the Ser1 field is the largest, and most of the other fields have insignificant extinction.

Henceforth we will use only these extinction-corrected R magnitudes.

2.7. Completeness Tests

Completeness estimation is straightforward because of the automated nature of the cataloging process. If we are interested in the detection efficiency f_i in image i for objects of a given magnitude and shape, we simply add objects with these properties into image i and run FOCAS exactly the same way as for the original catalogs. We then search the new catalog for detections within 1.5" of the locations of the artificial objects; f_i is then simply the fraction of the artificial objects which are recovered. Artificial objects which merge with brighter preexisting objects are not considered to be "recovered." These Monte Carlo tests give us the marginal detection probability f_i for objects with the chosen magnitude and shape—the probability that the next additional object would be detected.

We have conducted these Monte Carlo tests to obtain the completeness f_i vs. magnitude for stellar objects in each of the fields, with results shown in Figure 4. The Coma image is 50% complete for stars at R=25.5, and the control fields match this value to within 0.1 mag. Because the fields are well-matched and the f_i are very similar, the completeness corrections have only a second-order effect on the removal of background counts from Coma. At $R \sim 24$ the Coma field is less complete than the control fields because it contains many more large galaxies which obscure parts of the field. The very brightest of these we have either masked or subtracted away using elliptical isophote fits, but many R > 16 cluster members remain, and effectively "shadow" the R > 22 galaxies in which we are primarily interested. The Monte Carlo results for f_i are necessary to quantify this effective loss of area in the Coma field due to increased crowding. Note that the "bright" galaxies which cause the crowding have $M_R \lesssim -13$, well into the regime of what are normally denoted as dwarf galaxies. Our chief interest lies in yet fainter galaxies.

The Monte Carlo tests show that m_t is an unbiased estimator of true magnitude for stellar objects down to the 50% completeness level. The RMS error in magnitude for R = 25.25 stellar objects is 0.4 mag, with of course smaller errors at brighter flux levels.

We have also conducted extensive Monte Carlo tests using resolved objects instead of stellar objects. The techniques used are exactly the same as above; we will defer discussion of these results until later, when we investigate the sizes of Coma cluster galaxies.

3. Methodology of Differential Counts

3.1. Estimating Background Counts

We wish to use data from the 5 control fields to estimate the number of objects in the Coma field which are background or foreground to the Coma cluster itself. For brevity, we will henceforth use the word "background" to mean objects that are either foreground or background to the Coma cluster. We assume that the number of and detection efficiency for the background in the Coma field is *typical* of the control fields. In other words, the Coma *cluster* objects have simply been added into our catalogs atop the background typical of high latitude fields. If this is true, we may estimate the background counts in the Coma field by taking the mean of the control field counts. We may furthermore estimate the *uncertainty* in the Coma background counts from the variance of the control-field counts. In the next subsection we discuss ways in which the Coma field might have an atypical

background population or perhaps an atypical detection efficiency for background objects. First we give the formulae used to estimate the background and its uncertainty.

Consider a particular type of object—e.g. having detected magnitude within a certain range. We wish to estimate the number N_{bg} of these in the Coma catalog which are background as opposed to cluster members. Let the number of equivalent objects in the control fields be N_1, N_2, \ldots, N_M , where M = 5 is the number of control fields. Since N_{bg} is assumed to be drawn from the same population as the N_i , our best estimate for N_{bg} is simply the mean

$$\tilde{N}_{bg} = \frac{1}{M} \sum_{i=1}^{M} N_i \frac{A_C f_C}{A_i f_i}.$$
 (1)

We make corrections (of a few percent) to the counts N_i to correct the areas A_i and detection efficiencies f_i of the control fields to match A_C and f_C of the Coma field. Next we ask what will be the RMS deviation σ_{bg} of the actual N_{bg} from the estimate \tilde{N}_{bg} . The best estimate of this is given by

$$\sigma_{bg}^2 = \frac{M+1}{M(M-1)} \sum_{i=1}^{M} (N_i \frac{A_C f_C}{A_i f_i} - \tilde{N}_{bg})^2.$$
 (2)

In essence we have drawn M samples from some distribution, and ask how accurate our estimate of the next sample will be. Note that this is not the same as estimating the variance of the population, as is usually done, and hence we have an extra factor of (M+1)/M relative to the usual expression.

We can use Equations (1) and (2) to estimate the background counts in some magnitude bin, or in some joint magnitude- \mathcal{R} bin. The beauty of this technique is that error estimates are generated from the control fields, so we need not rely on models of our uncertainties. Background fluctuations due to Poisson statistics, galaxy clustering, magnitude zeropoint errors, mis-estimation of the f_i , etc., are all automatically included in σ_{bg} as long as the processes which generate these variations are operating similarly in the Coma field as in the control field. Thus we do not have to estimate or even be aware of the sources of error in the background correction, as long as these errors are the same in the Coma field as in the control fields.

3.2. Estimating Cluster Counts

If N_C objects are detected in the Coma field and \tilde{N}_{bg} is our estimate of the number of background objects, then the remainder

$$N_{det} = N_C - \tilde{N}_{bq} \tag{3}$$

is our best estimate of the number of detected cluster members. The uncertainty σ_{det} in N_{det} is equal to σ_{bg} , since there is no uncertainty in N_C . Next we wish to estimate the number N_{cl} of objects actually present in the Coma cluster within the solid angle of our field. We must correct for the detection efficiency f_C , so

$$N_{cl} = N_{det}/f_C. (4)$$

Finally we desire the uncertainty in this quantity, for purposes of fitting luminosity functions, etc. We assume that galaxies are placed into our field by a Poisson process (a cosmic variance of sorts), and that the detection process is also Poissonian. Then the final uncertainty in the parent cluster luminosity function is given by

$$\sigma_{cl}^2 = (\sigma_{bg}^2 + N_{det})/f_C^2, \tag{5}$$

where the first term is the background uncertainty and the second term accounts for the Poisson fluctuations of cluster counts. Note that the fluctuations in the background counts are already contained within σ_{ba}^2 .

3.3. Possible Pitfalls

Having many control fields allows us to make internal estimates of both the background and its variance for our program field, free of systematic biases, as long as the program field is not extreme in some way relative to the controls. There are, however, several ways in which the Coma field is extreme relative to the controls, and we must assure that these differences do not bias our results. Here we enumerate these potential pitfalls and their effects.

3.3.1. North Galactic Pole—Dust and Stars

The Coma field would be unique even without the presence of the Coma cluster because it lies near the North Galactic Pole, and thus suffers less Galactic dust extinction than the average control field, and is likely to have lower star counts as well. We have corrected for extinction as outlined in §2.6., which should alleviate the first problem. Differential star counts should not be a problem for R < 21 because we have excluded stars from the object counts as described in §2.5. For R > 21, stars are not readily distinguished from galaxies, so we do not attempt an exclusion of stellar objects because we do not want to be biased against compact galaxies in the Coma cluster. We expect, though, that the difference in star counts between the NGP and our control fields is small compared to our cluster signals. We have calculated the expected NGP star counts using the Galactic models of Ratnatunga (1993), and these are plotted in the lower panel of Figure 4 along with the total object counts. If the Coma field were to have fewer stars than the control fields, this would cause us to underestimate the Coma cluster galaxy counts in the 21 < R < 23 range.

3.3.2. Dust in the Cluster

The Coma field differs from the control fields in one other major respect, namely that there is a large galaxy cluster in the middle of it! The presence of the Coma cluster could alter the appearance of galaxies in its background in two ways. First, if there were dust in the cluster core, the background galaxy counts would be diminished. Romani & Maoz (1992) detect a deficit of quasars in Abell cluster fields, and posit an extinction of $E_{B-V} \sim 0.3$ in cluster cores as an explanation. Ferguson (1993), however, limits $E_{B-V} < 0.05$ in the Coma cluster based on the colors of elliptical galaxies. We assume zero extinction in the cluster. If there is dust in Coma, it reduces the number of observed background galaxies and again causes us to underestimate the number of cluster member galaxies.

3.3.3. Gravitational Lensing

The Coma cluster might also alter the appearance of its background population by gravitational lensing. The critical surface mass density in Coma for lensing of distant background galaxies is $\Sigma_c = c^2/4\pi GD = 3.5$ g cm⁻². A singular isothermal sphere with a 1-d velocity dispersion of 1000 km s⁻¹ has a surface mass density of $\Sigma = 0.24(r/100 \,\mathrm{kpc})^{-1}$ g cm⁻², where r is the distance from the core; if the cluster has a finite core radius r_c , the central surface mass density is obtained by setting $r = r_c$. Distant background objects will be magnified by a factor $(1 - \Sigma/\Sigma_c)^{-1}$ in area, which of course

increases the flux from each background galaxy (gravitational lensing conserves surface brightness). The cluster lens amplification, however, reduces the solid angle of distant Universe being viewed behind Coma by the same factor. If the background object counts per magnitude scale as $d(\log N)/dm = \alpha$, then the lensing will change the background counts by the factor $|1 - \Sigma/\Sigma_c|^{2.5(0.4-\alpha)}$. In the R band, $\alpha = 0.39$ (Tyson 1988), so we see that lensing will have a very small effect upon the background counts (in fact will decrease the counts) unless the surface density of Coma is near the critical value. To reach $\Sigma = \Sigma_c$ would require a core radius for Coma of $r_c \leq 7$ kpc, or 15" at the distance of Coma. Thus even in the very unlikely event that the Coma cluster is a critical lens, the critical region would subtend only a small part of our field, and furthermore the lensing would cause us to again underestimate the Coma cluster membership. We may safely ignore the effects of gravitational lensing!

3.3.4. Large-Scale Structure

One may worry that our estimate of the Coma cluster LF may be artificially inflated because the Coma field crosses the Great Wall, a large sheet-like concentration of galaxies in which the Coma cluster is embedded. While structures such as the Great Wall are not rare in the Universe, and hence may also be present in the control fields, the reader may be concerned that we are in fact measuring the LF of the Coma core *plus* a cross section of the Great Wall population. In §4.5., we find that the Coma field excess objects are strongly clustered on NGC 4874, indicating that the majority of these excess objects are probably true cluster members rather than superposed Great Wall members.

3.3.5. Diffuse Light Gradient

The Coma image has a very strong diffuse light gradient which is not present in any of the control field images. This might have two effects on the detection of background objects: first, the diffuse light contributes photon noise and surface-brightness-fluctuation noise to the Coma image which is absent from the controls. This could potentially affect the detection efficiency or false positive rate for faint objects. Calculations indicate that this effect is negligible, and this is borne out by the fact that artificial galaxies placed in the higher-noise part of the Coma image are detected with the same efficiency as identical galaxies placed in the lower-noise half.

The second effect of the diffuse light is more worrisome: it has forced us to perform an image processing step on the Coma image which was not performed on the control images, as described in §2.3.. The galaxy-fitting and median-filtering steps remove only long-wavelength signals from the image, and hence have little effect upon objects with angular sizes below 10". The control catalogs contain few or no faint background galaxies this large, so there is no bias in the Coma background galaxy estimate. It is possible, however, that the median filter has removed flux from extremely diffuse Coma cluster member galaxies, and therefore depressed the apparent number of Coma cluster members in our final LF. Our Coma catalog does become incomplete for faint LSB objects with scales $\geq 10'' \approx 5$ kpc because they are attenuated by the median filtering and FOCAS sky-subtraction; a few such objects are visible in the unfiltered Coma image. Proper study of these most diffuse objects in the Coma field requires a different approach to background removal, and we defer discussion of these objects to a later paper (Ulmer et al. 1995). Their numbers are small, however, and will not affect the conclusions of this paper.

3.3.6. Crowding

The Coma image has of course a much higher density of bright galaxies than any of the controls, leading to a lower faint-object detection efficiency for Coma because of the effective loss of area. As already discussed, we compensate for this crowding by first subtracting or masking the very brightest galaxies, and then running Monte Carlo tests to calibrate the "shadowing" effect of the remaining galaxies. Crowding affects the detected counts in a non-linear fashion, and hence when the density of faint objects in the Coma field greatly exceeds that in the control fields, it may be inaccurate to estimate the crowding effects through the addition of a few Monte Carlo galaxies at a time to the control images. A complete Monte Carlo simulation requires that we add to the control images an artificial version of the *entire* population of galaxies posited to exist in the Coma cluster, and note whether the Coma counts are recreated. We have implemented a few such full-population Monte Carlo tests, and the results are in agreement with those derived from the simpler, model-independent technique of estimating detection efficiencies by adding a few stars at a time to each image. We conclude that the simpler technique adequately accounts for crowding.

4. Magnitude, Size, and Spatial Distributions of Coma Cluster Members

In this section we apply the methodology of §3 to the catalogs described in §2, deriving the luminosity function and typical sizes of galaxies in the Coma cluster. We also investigate the spatial distribution of the very faint cluster members.

4.1. Magnitude Distribution

We may apply Equations (1) through (5) to the numbers N_i of objects with a given range of magnitudes to obtain an estimate of the number N_{cl} of cluster members in that magnitude bin. In Figure 4 we plot the Coma counts N_C vs. R magnitude, alongside the estimate and uncertainty \tilde{N}_{bg} and σ_{bg} of the background counts derived from the control field. Also shown in Figure 4 are the expected numbers of background galaxies and Galactic stars. The Coma counts significantly exceed the control-field counts at almost all magnitudes down to our completeness limit, as seen in Figure 4.

In applying Equations (1) through (5) to the data in a given magnitude bin we use for f_i the detection efficiency derived for *unresolved* objects at that magnitude. Coma cluster members could be resolved and have somewhat lower detection efficiencies; hence our derived values of N_{cl} may be low estimates of the true population near the limiting magnitude of the image. The 50% completeness magnitude for exponential-profile galaxies of various scale lengths is plotted in Figure 7.

In Table 2 we give the gross counts N_C , background \tilde{N}_{bg} , net N_{det} , and completeness-corrected counts N_{cl} in each magnitude bin. Figure 5 plots as filled circles the derived N_{cl} vs. R magnitude, the Coma cluster luminosity function (LF). Parameterizing the LF as a power law $dN/dL \propto L^{\alpha}$, two regimes are apparent: for R < 23.5 ($M_R < -12.4$), the LF is consistent with the $\alpha \approx -1.3$ range that the deepest previous cluster LF studies have found (Sandage, Binggeli, & Tammann 1985, SBT). For R > 23 ($M_R > -12.9$) we find a much steeper LF, with $\alpha \approx -2$. At these magnitudes, however, it is possible that Coma cluster globular clusters are being detected as well as Coma cluster galaxies. We will therefore defer further discussion of the Coma cluster galaxy LF until the next section. We first investigate the characteristic sizes and the spatial distribution of the detected Coma cluster members, which will help in distinguishing galaxies from globular clusters.

4.2. Extension to Bright Galaxies

The brightest galaxies in the Coma field are saturated on our CCD images, and furthermore there are few bright galaxies in our small field. In order to extend our LF measurement to brighter limits, we have used the catalog of Godwin, Metcalfe, & Peach (1983, GMP83), who have digitized b- and r-band 2.5° square photographic images of the Coma cluster. Their published galaxy catalog is complete to b = 21, and thus we can use it for galaxies r < 18 without danger of incompleteness. For the 21 unsaturated galaxies in our catalog with R < 19, a fit for a magnitude offset between our and the GMP83 photometry yields $R = r + 0.29 \pm 0.17$. We use this to convert the GMP83 r magnitudes into our R system. The surface density of galaxies differs across the face of the Coma cluster, and we want to generate a bright-galaxy LF which is directly comparable to our CCD field, so we must sample the GMP83 data at comparable distances from the Coma center as our CCD data. We generate a LF from the GMP83 sample using only the galaxies within 8' of NGC 4874. The CCD field consists essentially of one quadrant of this circle. As a background region for the GMP83 8' target sample we use an annulus at $1^{\circ} < r < 1.25^{\circ}$ from NGC 4874. The density of galaxies in this annulus is <20% of the density inside the 8' circle, so we need not be too concerned about whether this background annulus contains cluster members. We subtract the background galaxy density from the target galaxy density and multiply by the area of the CCD field to obtain bright-galaxy counts to compare with the CCD counts. Uncertainties are derived from the square root of the target-field counts. The GMP83 galaxy counts are plotted as the open circles in Figure 5, and are listed in Table 3. The agreement between the CCD data and the GMP83 data is good in the region of overlap. In this way we obtain a LF for Coma cluster members for the range 10 < R < 25.5, spanning more than 6 decades in luminosity!

4.3. Are the Faint Objects Resolved?

Previous observations of faint objects near NGC 4874 have found globular clusters as bright as $B \sim 24$ (TV87; Harris 1987), and have yielded hints of a population of resolved objects as well. Recent HST observations may have observed globular clusters as bright as V = 24.2 near NGC 4881, another Coma cluster giant elliptical galaxy (Baum *et al.* 1994). This suggests that the excess objects in our Coma field may include globular clusters at $R \gtrsim 23.5$ as well as dwarf galaxies. Our PSF FWHM of 1.3" subtends 600 pc at the distance of Coma, so the globular clusters would be unresolved in our images, while the dwarf galaxies may or may not be resolved. In order to determine the possible extent of globular cluster contamination in our LF, and to determine the size range of our dwarf galaxies, we investigate the distribution of the resolution parameter \mathcal{R} for our excess galaxies.

When determining the Coma cluster LF, we did not actually attempt to assign cluster membership to individual objects, but rather used a statistical method to determine the overall number of cluster members. Likewise, for R > 21, it is impossible to unambiguously determine the degree of resolution of each individual object. This is because the distribution of \mathcal{R} for unresolved objects begins to overlap the \mathcal{R} distribution for galaxian objects. We can, however, determine the degree of resolution for the entire population by comparing the observed distribution of \mathcal{R} to the distribution expected for a population of unresolved objects.

In Figure 6 we plot the distribution of \mathcal{R} for the Coma cluster objects in each of six magnitude slices. These histograms were derived in exactly the same way as the luminosity function: we count, for example, the number N_C of objects in our Coma catalog having 23.5 < R < 24.0 and $1.0 < \mathcal{R} < 1.25$. We likewise count the numbers N_i of objects in this range of R and R in each of the control catalogs. The methods of §3 are then used to derive the number N_{det} and uncertainty σ_{det} of detected excess objects in this joint magnitude-resolution bin. This process is repeated over a two-dimensional grid of R-R bins, with the results shown in Figure 6 as the histograms with error bars.

Also shown in Figure 6 as the dotted curves are the distributions in \mathcal{R} that would be expected if all the excess counts were unresolved. The \mathcal{R} distributions for unresolved objects are obtained from the Monte Carlo simulations. The PSF template used for the Monte Carlo unresolved objects is a Moffat function, which has $I(r) \propto (1 + r^2/r_0^2)^{-\beta}$. The two parameters β and r_0 are adjusted to force both the FWHM and the second-moment radius to match those of bright stars in the Coma image.

It is immediately apparent from the first two panels of Figure 6 that in the 22.5 < R < 23.0 and 23.0 < R < 23.5 magnitude ranges most of the Coma excess consists of resolved objects. Indeed we can make a conservative estimate of the number of galaxies in these magnitude bins by counting the objects with $\mathcal{R} > 1$, since we do not expect any unresolved objects to be detected with such large \mathcal{R} values. Our estimates of the number N_{res} of resolved objects are shown in Table 2, and are plotted as the open triangles in Figure 5. The great majority of objects in these two bins are seen to be resolved by this simple test, or by other, more sophisticated, tests. The same holds true in all brighter magnitude bins, which are not plotted.

Note that the uncertainties in the number of definitively resolved objects ($\mathcal{R} > 1$) are smaller than the error bars on the total number of objects. This is true because most of the variance in background counts at these magnitude ranges is for unresolved or marginally resolved objects ($\mathcal{R} < 1$). This is partially due to the fact that cluster dwarf galaxies tend to be more diffuse than background galaxies, a fact well known to the many astronomers (such

as SBT85) who have sought dwarf galaxies in more nearby clusters using morphological criteria. The agreement apparent in Figure 5 between our resolved counts (open triangles) and the overall counts (filled circles) is reassuring evidence that there are not large numbers of compact dwarf galaxies in the Coma cluster for $M_R \lesssim -12$. This is good news if true in Virgo and Fornax as well, because it means that there are not large numbers of high surface brightness dwarfs that SBT85 and Ferguson & Sandage (1988, FS88) would have missed in their morphologically selected cluster LF's.

In the next fainter bin, 23.5 < R < 24.0, there is a tendency for the detected Coma cluster objects to have \mathcal{R} greater than expected of unresolved sources, but the data are consistent with an unresolved population at a one-sigma level so we cannot reject this hypothesis. Likewise we find that the \mathcal{R} histograms in all of the fainter bins are consistent with a population of unresolved objects.

We cannot conclude, however, that all of the excess objects with R > 23.5 are globular clusters. As we near our completeness limit of R = 25.5, several factors conspire to make it difficult to distinguish between galaxies and globular clusters: first, the detected galaxies at R < 24 are clearly becoming smaller as their luminosities decrease—note that in the first three panels of Figure 6, the peak of the \mathcal{R} histogram is moving toward the left (less resolved). If we extrapolate this apparent size-luminosity relation, we find that for R > 24, we expect most of the dwarf galaxies to be too small to resolve.

At fainter magnitudes, the S/N of our detections is getting too low to permit much discrimination as to their size. Monte Carlo tests show that for R > 24.5 it becomes essentially impossible to distinguish a population of stellar objects from a population of objects 1.5–2 times as large as the PSF. Objects significantly more extended become seriously incomplete at these magnitudes, as they fall below the surface brightness threshold of our detection process. Thus for R > 24.5 the \mathcal{R} histogram will always be indistinguishable from that of an unresolved population due to S/N limitations.

The most direct evidence that many of the excess R < 25 objects must be galaxies is given by TV87, who have imaged at 0.6" FWHM resolution a field located 40" W of NGC 4874. They use a field 340" away from NGC 4874 as a "reference" field, though in fact this second field is within our larger Coma image¹. In the magnitude range 25.25 < B < 26.25, corresponding roughly to 24 < R < 25, TV87 report approximately 30 more objects in the inner field than in the reference field. Of these, roughly one-third are

¹As a cautionary note, we point out that the "prominent dwarf galaxy with many subcondensations" within the TV87 reference field is completely absent in our deeper image. Ghost images are easily confused with very extended galaxies.

resolved and are denoted by TV87 as a "retinue of dwarf galaxies" near NGC 4874. The remainder are unresolved and are assumed to be globular clusters. This suggests that a substantial fraction of the 23.5 < R < 25 objects in our field are in fact galaxies which we cannot resolve.

To summarize, examination of the distribution of the resolution parameter \mathcal{R} for the excess objects gives unambiguous evidence that we may consider the great majority of the R < 23.5 ($M_R < -11.4$) excess counts to be galaxies. For R > 23.5, we cannot identify a resolved population, but external evidence suggests that a substantial fraction are dwarf galaxies while globular clusters could easily comprise the majority.

4.4. Size Distribution of Coma Cluster Galaxies

We may use the observed \mathcal{R} distributions to determine a characteristic size for the Coma cluster dwarf galaxies as a function of magnitude. As a means of quantifying the sizes of these dwarfs, we will assume that they have exponential surface-brightness profiles,

$$I(r) = I_0 e^{-r/r_s},\tag{6}$$

and circular symmetry. Of course we have little information on the profiles of the extreme dwarf galaxies in our images. The best-studied galaxies of similar luminosities are the Local Group dwarf spheroidals, which are well described by exponential profiles, so for ease of comparison we adopt this function. Indeed almost all faint dE galaxies are satisfactorily fit by exponentials (FB94; Impey, Bothun & Malin 1988).

We perform Monte Carlo tests to determine the distributions of detected magnitude and \mathcal{R} to be expected if galaxies of a given luminosity and r_s are present in the Coma cluster. The IRAF task ARTDATA is used to add artificial seeing-convolved exponential galaxies onto the Coma image, and the methods described in §2.7. are used to determine the detection efficiency and expected parameter distributions. We can then see if exponential-profile galaxies with the selected magnitude and r_s are present in Coma by noting whether this Monte Carlo distribution of R and R overlaps significantly with the Coma R–R distribution in Figure 6.

The results of these comparisons are shown in Figure 7. We restrict our attention to the faintest objects in our CCD frame. For the 22.5 < R < 23.0 bin, corresponding to $M_R = -12.2$, we find that the Coma galaxies' scale lengths are in the range $250\,\mathrm{pc} < r_s < 450\,\mathrm{pc}$. Objects 0.5 mag fainter are about a factor 2 smaller. This range of

detected galaxy sizes is shown as the heavily shaded region in Figure 7. For galaxies fainter than $R \approx 23.3$ ($M_R > -11.6$), our detections are not meaningfully resolved. The lightly shaded region in Figure 7 denotes the magnitudes and scale sizes that could potentially exist in the Coma cluster as part of our unresolved detections—this region extends to zero size, of course. Finally, the heavy line shows the locus at which our detection efficiency is 50%. Galaxies rightward of this line would likely have escaped detection by us. In producing Figure 7 we have made corrections for the tendency for FOCAS to underestimate the flux from exponential-profile objects, so that the magnitude scales refer to actual rather than detected magnitude.

Only in the Local Group is comparable information available for galaxies this faint. The 10 Local Group dwarf spheroidal galaxies for which scale lengths and magnitudes are available are plotted on Figure 7 as they would appear at the distance of the Coma cluster (the Fornax galaxy is too bright to appear on this plot). These data are primarily from Caldwell et al. (1992), and we have assumed V - R = 0.5 for the dSph's. We note first that 7 of these 10 galaxies would have been detected in our images if they were placed in the Coma cluster. Second, we note that the sizes of the Coma cluster dwarf galaxies are similar to Local Group dSph's of comparable magnitude.

The observed size distribution of Coma cluster members does not abut the detection threshold for R < 24. In other words, we have found a minimum to the central surface brightness of galaxies. We are thus unlikely to be missing significant numbers of R < 24 galaxies due to surface brightness selection effects, unless of course there is an entirely disjoint population of objects lurking beneath our surface brightness threshold of ≈ 27.6 mag arcsec⁻².

4.5. Radial Distribution of Coma Cluster Members

Information on the spatial distribution of different types of cluster members could be important in determining their natures and histories. Examination of Figure 2 suggests that the object density in Coma increases markedly toward NGC 4874, and indeed a measurement of the object density as a function of the distance r from the center of NGC 4874 shows a significant gradient for all types of objects. We bin the detected objects in the Coma field into several annuli around NGC 4874, and calculate the fraction a of the entire useful field that lies within each annulus. The background estimates \tilde{N}_{bg} from the control fields are scaled by a to give an estimate of the background in each annulus, and we scale σ_{bg} by \sqrt{a} to estimate the uncertainty in the background within each annulus. We

then calculate the object density above background in each annulus of the Coma image. These excesses are shown as a function of r for the magnitude range 20.5 < R < 22.5 as squares in Figure 8. The starred symbols in Figure 8 show the radial gradient for our 22.5 < R < 23.5 objects; these are the faintest objects which we can reliably label as galaxies. The open circles in Figure 8 show the radial gradient of the 23.5 < R < 25.5 Coma objects, which may be predominantly globular clusters. In each magnitude bin we actually plot the mean surface brightness above background contributed by Coma cluster members. No incompleteness corrections have been made, so the surface brightness in the faintest bin may be underestimated by a few tenths of a magnitude.

Also plotted in Figure 8 is the strength of the Coma cluster diffuse light signal visible in Figure 1. The hatched area reflects the uncertainty in our knowledge of the background diffuse brightness level. At one extreme we have assumed that the SE corner of our image, 10' from NGC 4874, contains zero diffuse cluster light. The upper bound of the hatched region shows the diffuse light signal obtained by assuming that the $r^{-1.3}$ power-law gradient in diffuse light seen in the NW corner of our image extends to r = 10'. The dotted lines in Figure 8 all trace $r^{-1.3}$ power-law profiles, for reference.

Finally we have included in Figure 8 the radial profiles of the light provided by galaxies in the GMP83 catalog, divided into 14 < b < 17.5 and 17.5 < b < 21 magnitude bins. The error bars on these points also arise from our uncertainty in the background galaxy density. We must derive the background density from the $0.9^{\circ} < r < 1.1^{\circ}$ annulus of the GMP83 catalog. The error bars on the plotted points are the bounds obtained by assuming that between 10% and 90% of the counts in this outer annulus are due to background galaxies.

Several conclusions may be drawn immediately by inspection of Figure 8. Foremost, we see that the excess counts we detect in Coma show a highly significant gradient toward NGC 4874 at all magnitudes. This is very strong evidence that our excess counts are in fact due to objects present in the Coma cluster. If our excess counts were an artifact of some background subtraction error (e.g. one of the pitfalls mentioned in §3), then we would not expect to see this gradient. Similarly, if the excess were due to Great Wall objects not physically associated with the Coma cluster, we would not expect a concentration about NGC 4874.

Our next immediate conclusion is that the dwarf galaxies and globular clusters contain little of the total luminosity of the cluster. Within the 1' < r < 10' region spanned by our CCD field, we see that the total diffuse flux is similar to the flux from bright galaxies in the cluster. What would normally be called "dwarf" galaxies, with 17.5 < b < 21, contribute ≈ 1.5 mag less light at $r \gtrsim 5'$, while the extreme dwarfs from our CCD image (R > 20.5) and globular clusters produce 6–7 mag less light than the diffuse light or giant galaxies.

Unless these extreme dwarfs have mass-to-light ratios several hundred times larger than the giant galaxies, they do *not* contain a major fraction of the cluster mass.

We note also that the radial density gradient differs for various classes of objects. Parameterizing the surface brightness as proportional to r^{β} , we find that the diffuse light is best fit by $\beta = -1.3 \pm 0.1$. The same $\beta = -1.3$ power law is a good fit to both magnitude slices of the GMP83 catalog for r > 5', but the "dwarf" galaxies at 17.5 < b < 21 show a significant flattening of the density for r < 5'. This conclusion was also reached by Thompson & Gregory (1993), who report a drop in density of dwarf spheroidal galaxies for r < 20', and a somewhat milder flattening for their "very faint dE" sample at $b \approx 20.5$. We have not subdivided our objects by morphology, but there seems to be general agreement. Thompson & Gregory suggest that their dSph galaxies are being destroyed by the cluster tidal field. It is thus interesting to see if the central deficit persists to yet fainter galaxies. In fact we find that the squares in Figure 8, representing our 20.5 < R < 22.5 dwarfs, follow a $r^{-1.3}$ power law for r > 1.5', but are significantly depleted for r < 1.5'; this turnover radius is quite a bit smaller than the $r \approx 5'$ at which the GMP83 galaxy density (filled triangles) flattens out. Note that our results for the radial gradients of dwarf galaxies are quite similar to the results of Vader & Sandage (1991), who find a dwarf density $\propto r^{-1.22}$ in the vicinity of RSA elliptical galaxies. Their data show a deficit of dwarfs relative to this power law for projected radii less than $50h^{-1}$ kpc, which would correspond to 2.4' at the distance of the Coma cluster. The Vader & Sandage dwarfs are selected on a morphological basis, but would correspond roughly to a 17–20 R magnitude range if placed in the Coma cluster. Zaritsky et al. (1993) find 69 satellites of 45 spiral field galaxies, and find the projected surface density of satellites drops as $r^{-1.0\pm0.2}$ within 300 kpc of the primaries. This is consistent with our population about NGC 4874.

The faintest objects in our images follow a $\beta \approx -1.3$ density gradient over our entire field. The starred symbols in Figure 8 show the run of density with r for the faintest objects which can confidently be called galaxies, 22.5 < R < 23.5. The open circles, for 23.5 < R < 25.5 objects, also are close to a $\beta = -1.3$ line, so that these fainter objects—be they $M_R > -11$ galaxies or globular clusters—share the steep gradient of the diffuse light. If tidal destruction is the cause of the central hole in the Thompson & Gregory dwarf spheroidal density or the central plateau in the 17.5 < b < 21 galaxy density, then the fainter galaxies we detect must be more robust to tidal stress. The plateau region becomes smaller for fainter galaxies, and is entirely absent for $M_R > -12$ galaxies in our data. We will consider the tidal stability of our objects in the next section.

Any concentration of objects toward the x-ray centroid of the cluster is at least 10 times weaker (2σ upper limit) than the concentration toward NGC 4874. Indeed the x-ray

emission itself peaks on NGC 4874, though the x-ray isophotes are quite asymmetric, being stretched toward NGC 4889. The x-ray brightness gradient within several arcmin of NGC 4874 is extremely weak, with $\beta \approx -0.15$ (Dow & White 1995). The strong peak in faint galaxy density and diffuse red light towards NGC 4874 thus lies inside a much flatter x-ray gas distribution.

We have searched for any tendency for the density of faint Coma cluster members to increase near the locations of bright galaxies other than NGC 4874. In particular we ask whether there is any concentration of objects toward the 10 brightest E/S0 galaxies in our field (excluding NGC 4874). For distances of 24" to 120", we find no change in density of 22 < R < 25.5 objects. Our sensitivity is such that a 20% change in the density of Coma cluster members would be noticed. Within 24" of the E/S0 galaxies we note a 2σ decrease in faint galaxy density; given the possible completeness problems this close to a bright galaxy and the poor statistics, we do not consider this significant. It thus appears that the number of globular clusters or dwarf galaxies which are bound to the generic giant galaxies in the cluster is small compared to the number bound to the potential well surrounding NGC 4874. An interesting exception is the tight subcluster of galaxies visible on the left side near the lower edge of Figures (1) and (2). The bright S0 galaxy in this subcluster is indeed a cluster member with cz = 7895 km s⁻¹ (Mazure et al. 1988); it would be worthwhile to obtain redshifts for the other galaxies in this apparent clump, which are redder than the central S0.

5. The Galaxy Population of the Coma Cluster Core

In this section we take a closer look at what the data presented above tell us about the galaxies found in the core of the Coma cluster, particularly with reference to results on very faint galaxies in other environments. We will work primarily with absolute magnitudes and sizes rather than apparent units. As a reminder, if we parameterize the Hubble constant as $H_0 = 75h_{75}$ km s⁻¹ Mpc⁻¹, we are assuming $h_{75} = 1$. For other Hubble constants, luminosities scale as h_{75}^{-2} and sizes scale as h_{75}^{-1} .

5.1. Luminosity Function for Galaxies $M_R < -11.4$

Our first task is to determine the slope of the faint end of the galaxy LF. We fit power laws of the form $dN/dL \propto L^{\alpha}$ to the N_{cl} data in Tables 2 and 3 with $-19.4 < M_R < -11.4$.

The bright limit of the fit is chosen to be a few magnitudes below the canonical L^* for clusters (e.g. Lugger 1986), placing us on the power-law part of the LF. This also sidesteps the vagaries of small-number statistics at the very bright end. We are fitting only toward the faint side of the possible "hole" in the Coma cluster LF at b=17.5 ($M_R\approx-19$) reported by Biviano et al. (1995). We do not attempt to fit faintward of R=23.5 since globular cluster contamination may be a problem there. We use the resolved-count estimates N_{res} for 21 < R < 23.5 rather than the total counts N_{cl} . While this introduces a morphological bias against compact dwarf galaxies, it reduces the uncertainties. If we instead fit to the N_{cl} we get results that are completely consistent, albeit with slightly larger errors. Likewise we obtain consistent results whether or not we include the photographic data at the bright end.

Least-squares fitting over this range yields $\alpha = -1.42 \pm 0.05$, with a χ^2 value of 7.2 for 9 degrees of freedom. This power law, shown as the solid line in Figure 5, is thus completely consistent with the data. The 95% confidence interval is $-1.57 < \alpha < -1.25$. These α values are consistent with those derived for Coma by Biviano *et al.* (1995) and by Thompson & Gregory (1993), who each conduct much shallower ($M_R \leq -16.5$) but wider-area surveys of this cluster.

This α is compatible with most results on the faint-end slopes of cluster LFs, or of dE galaxies in clusters. An overview of previous results is in FB94; here we update this discussion in light of our results. The most extensive previous measurement of the LF of a galaxy cluster is that of SBT85, who have selected Virgo cluster members on a morphological basis to a limit of B = 18. Assuming a Coma/Virgo distance ratio of 5.5, and a typical B-R color of 1.3 for dwarf galaxies, this limit corresponds to $M_R=-14.4$ with our assumed H_0 . To this depth, SBT85 derive an overall LF with $\alpha = -1.25$ (no uncertainties given). A slightly steeper slope of $\alpha = -1.30$ is fit to incompleteness-corrected counts to B = 20 ($M_R = -12.4$). A fit to our Coma counts over the $-19.4 < M_R < -12.4$ region yields $\alpha = -1.32 \pm 0.07$, with $\chi^2 = 3.32$ for 7 degrees of freedom. Thus our Coma LF has a very similar shape to the SBT85 Virgo LF at the faint end. Various morphological subsets of the SBT85 data are fit with faint-end slopes of $-1.45 < \alpha < -1.35$; we have not made morphological distinctions, but still measure similar slopes at very faint magnitudes. FS88 measure the Fornax LF to similar depth as the SBT85 Virgo study—the overall LF slope in Fornax is consistent with the Virgo and our Coma results. Several caveats are in order, however, before we happily conclude that all clusters have $\alpha \approx -1.4$ at the faintest measured magnitudes.

5.1.1. Very Steep Cluster Luminosity Functions?

De Propris et al. (1995) have recently reported very steep faint-end LFs in several rich Abell clusters. In particular, they fit $\alpha = -2.2 \pm 0.2$ to A2199 galaxies with $-15.5 < M_B < -10.5$, corresponding for typical dwarf colors to $-16.8 < M_R < -11.8$. This differs by many sigma from our results for similar galaxies in Coma. De Propris et al. report similarly steep slopes for the I-band LF of three other clusters. Such dramatic differences between the Virgo and Coma clusters on the one hand, and A2199 on the other, deserve further investigation. These authors lack sufficient control field coverage and were forced to use galaxy counts from the literature to correct for background. It would take a rather large error in background correction to bring their LF slope into agreement with ours, but counts of background galaxies are notorious for varying when measured by different investigators. These authors have repeated their measurements with more extensive background observations and we await their results.

Driver et al. (1994) measure the R-band LF of the z=0.206 cluster A963, to a limit of $R\approx 24.5$, which corresponds to $M_R\approx -16$. The overall slope of the A963 LF over the $-21 < M_R < -16$ range is $\alpha\approx -1.5$, not greatly different from our lower-redshift Coma data. These authors prefer to interpret their data as the sum of two populations, one with $\alpha=-1.0$ and another with $\alpha=-1.8$, but no other data are available in this cluster to support a distinction into two populations.

5.1.2. Varying Dwarf/Giant Ratios

If different galaxy types have distinct faint-end LF slopes, then the faint-end slopes of overall LFs in different environments could vary due to changes in the mix of galaxy types. In cases where the morphologies of the dwarf galaxies are known, one may fit LFs to the distinct types. SBT85 fit Schechter functions to various types of Virgo dwarfs, obtaining faint-end slopes in the range -1.35 to -1.45. FS88 conclude that while the overall LF in Fornax resembles that in Virgo, the dE population in Fornax has a significantly shallower slope ($\alpha = -1.09 \pm 0.09$) than in Virgo. Ferguson & Sandage (1991) further investigate the dwarf population in various nearby environments, and posit a general rule that the early-type dwarf-to-giant ratio increases significantly with cluster richness. While we do not have morphological types against which to test this relation, Ferguson & Sandage (1991) offer another formulation of this hypothesis, which states that the ratio of faint $(-17 < M_R < -15)$ galaxy counts to bright $(M_R < -18)$ counts also increases with cluster

richness. Our data indicate that this ratio is lower in our portion of the Coma cluster than in the Virgo cluster, which would counter the posited relation. A more effective demonstration of this is given by Thompson & Gregory (1993), who have morphological information for nearly the entirety of the Coma cluster galaxies with $M_R \lesssim -16.5$. They conclude that the early-type dwarf-to-giant ratio in Coma is no higher than in Virgo.

5.1.3. Radial Variation of Luminosity Function

Another caveat to the direct comparison of Figure 5 with the SBT85 and similar data is that we image only the central portion of the Coma cluster. If the LF varies with radius from the cluster center, then our cluster core LF differs from the LF of the cluster as a whole. Thompson & Gregory (1993), for example, suggest that certain types of diffuse dwarf galaxies are deficient near the center of Coma. Figure 8 also suggests that galaxies with luminosities in the LMC range ($-17.4 < M_b < -14$) may be less concentrated on NGC 4874 than either brighter or fainter galaxies, which roughly follow a $r^{-1.3}$ density gradient over the range in which we measure them. In the Virgo cluster, the faint galaxies seem to be well mixed with the giant galaxies (FB94). Would we measure a different α if we were to survey the entire Coma cluster for $M_R < -11.4$ dwarfs? Examination of Figure 8 suggests that the LF for the entire cluster would, if different, be shallower than our derived $\alpha = -1.42$ were we to include more peripheral regions of the Coma cluster.

We check for radial variation of the LF by splitting our CCD field into two equal-area regions, one with r < 5.4' and the other r > 5.4'. In each half we count the number of resolved objects $(\mathcal{R} > 1)$ in bins spanning 15.5 < R < 23.5. We scale the background counts by one half and the background uncertainties by $1/\sqrt{2}$, correct for incompleteness, and fit to power-law LF's as for the full sample. We find that for the inner half of the field (r < 5.4'), $\alpha = -1.50 \pm 0.08$, with a 95% confidence interval of $-2.0 < \alpha < -1.2$. For the outer half of the field, $\alpha = -1.25 \pm 0.11$, with a 95% confidence interval of $-1.6 < \alpha < -0.5$. The fitted LF is shallower at greater distances from NGC 4874, but this is a weak signal. In fact both halves of the field are consistent with the $\alpha = -1.42$ determined from the entire sample. We do not detect any significant change in LF across our field, but the test is rather weak. The recent observations by Secker & Harris (1994) should, when fully reduced, give a more definitive answer to the question of radial dependencies in the LF in Coma.

There is growing evidence that surface brightness selection effects have an important impact on measurements of the LF in various environments. Ferguson & McGaugh (1995) demonstrate how a single galaxy population can potentially be responsible for the variety of measured α values in the field, as various surveys have distinct surface brightness thresholds. Sprayberry et al. (1995) construct a field LF from a galaxy survey with low surface brightness threshold, and likewise find that inclusion of LSB galaxies changes the LF significantly. Measurements of cluster galaxy LFs are not immune to surface brightness selection effects. We show here, however, that our Coma LF measurement is, for the reasons mentioned in the introduction, much less susceptible to surface brightness biases than previous works.

Each survey has a bounded region of sensitivity in the surface brightness vs. absolute magnitude (μ, M) plane. In deriving their Virgo LF, SBT85 corrected for insensitivity to LSB objects by noting a correlation of surface brightness with absolute magnitude in the complete region of this plane, and extrapolating into the incomplete region. Impey, Bothun, & Malin (1988) conducted a further survey of Virgo dwarfs using photographic amplification, and uncovered 26 new potential LSB Virgo dwarfs, most occupying regions of the (μ, M) plane inaccessible to SBT85. They repeat the SBT85 extrapolation, this time to lower central surface brightness of $\mu_0 \approx 26$ in B, and suggest that $\alpha = -1.7$ in a range comparable to our $-17 < M_R < -13.5$ (no error cited). After a further study of Fornax dwarfs, Bothun, Impey, & Malin (1991) attempt extrapolation into unexplored regions of the (μ, M) plane using a slightly different method: they assume that the LF is a separable function of scale length r_s and central surface brightness μ_0 , and derive $\alpha = -1.6 \pm 0.2$. This result is consistent with our Coma result (and with the SBT85 result, formally), but it does inspire us to assess our SB biases.

Two kinds of SB bias are possible: firstly against *high* SB galaxies which are missed in morphologically-based surveys due to their resemblance to foreground stars or background giant galaxies. We are free of such biases because we (initially) imposed no size restrictions on our counts. As previously discussed, our results do not change significantly when we restrict ourselves to resolved objects, and we thus conclude that there are few high SB dwarfs in the Coma cluster.

The survey is inevitably biased against low SB galaxies which are so extended as to fall below the SB threshold of the detection process. It is difficult to define a single SB threshold for our images, because the detection process for very extended objects is not limited by photon noise, but rather by the gradients in the diffuse cluster light. We do, however, have a surface brightness threshold well below any of the Virgo or Fornax studies—the detection isophote is nominally 27.6 R mag arcsec⁻², whereas the limiting isophote for the Impey,

Bothun, & Malin (1988) study is $\mu \lesssim 27~B$ mag arcsec⁻². In a more rigorous test of our sensitivity to LSB objects, we place artificial versions of exponential-profile galaxies on the Coma image and see if they survive the sky subtraction and detection process. Most of the galaxies detected via photographic amplification in Fornax have $r_s \lesssim 10''$ and $B \lesssim 20$; these galaxies would appear as $r_s \lesssim 2''$, $R \lesssim 22.7$ in our Coma data. Monte Carlo tests show that we would detect at least 75% of them, although the diffuse-light subtraction and FOCAS local sky determination lead to as much as 1.5 mag underestimate of their luminosity. The incompleteness is primarily due to crowding rather than noise. Likewise Impey, Bothun, & Malin (1988) find in Virgo a few galaxies with scale lengths as large as 30'', at $B \lesssim 17$. Such objects, if present in the Coma cluster, would be immediately visible in Figure 2, and would be efficiently detected, albeit with significant lost light.

We thus believe that we are capable of detecting galaxies at much lower central SB than in previous photographic surveys of clusters. We do not find the galaxy population filling the (μ, M) plane to the faint- μ limit of our detection region, except for the faintest galaxies as depicted in Figure 7. In other words, there does seem to be a locus of maximum galaxy density in this (μ, M) plane, and it is well within our detection region for $M_R < -12$. The existence and tightness of a correlation between μ and M for dE galaxies is under current debate (see FB94), and our extremely deep CCD images with wide dynamic range may help settle this question, at least as regards the Coma cluster. We defer further discussion of this question, however, to the succeeding paper (Ulmer et al. 1995), because the analysis of the most extended galaxies in our image requires us to remove diffuse light in a different manner.

We conclude that our LF is less subject to SB biases than any previous effort because the image has such low noise. While our algorithms underestimate the luminosities of the most diffuse objects, we find few objects large enough to be significantly affected in this way. This paucity of very large objects could be due to tidal destruction in the cluster, but in any case we do not detect many galaxies abutting the low-SB edge of our detection thresholds for $M_R < -12$.

5.2. Galaxies and Globular Clusters with $M_R > -11.4$

As seen in Figure 5, the Coma LF rises dramatically for $M_R > -11.4$ with a slope of $\alpha = -2$. Other investigators are reporting such upturns in cluster LFs, though at brighter magnitudes than this (De Propris *et al.* 1995). How much of the upturn in object counts faintward of $M_R = -11.4$ is attributable to globular clusters? Is it possible that the Coma

galaxy LF indeed turns sharply upwards at these magnitudes? If the number of globular clusters is negligible for $M_R < -9.5$, then the galaxy counts for $-12.5 < M_R < -9.5$ are indeed best fit by a power law of index $\alpha = -2.0$. If we assume to the contrary that the $\alpha = -1.43$ power law fit to the $M_R < -11.4$ data continues to describe the galaxy population at fainter levels, we would predict that one third of our detections in the $-11.4 < M_R < -10.4$ magnitude range were galaxies, with the remainder globular clusters. As mentioned in §4.3., TV87 indeed resolve about one third of the suspected Coma cluster members in this magnitude range, using a small image with 0.6" FWHM seeing. This is consistent with the $\alpha = -1.4$ extrapolation, but does not of course rule out the existence of numerous extra dwarf galaxies too small even for Thompson & Valdes to resolve.

An independent estimate of the number of globular clusters expected in our image can be made by assuming that the NGC 4874 globular cluster system is a scale model of the M87 globular cluster system observed in detail by McLaughlin, Harris, & Hanes (1994, MHH94). We first assume that NGC 4874 is 5.5 times more distant than M87, which makes it 1.7 times more luminous in V (de Vaucouleurs et al. 1991). MHH94 tabulate the number of globular clusters by observed V magnitude; assuming V - R = 0.5 on average (Hopp, Wagner, & Richtler 1995), we may transform the M87 V magnitudes to Coma-distance Rmagnitudes by adding 3.2 mag. If the specific frequency of globular clusters is similar to that of M87 (which is quite rich in globular clusters), then there will be 1.7 times more total globular clusters around NGC 4874 than M87. We lastly need to correct for the fact that MHH94 count globular clusters within a 6.8' radius of M87 (which would be only 1.2' at the distance of Coma), while our field spans a more extensive region around NGC 4874. We will assume that the surface density of globular clusters drops as $r^{-1.3}$ with distance from NGC 4874, since this is the behavior we observe for the faintest objects in our field. It is furthermore consistent with the radial gradients observed near M87 by MHH94, and with the $r^{-1.39\pm0.15}$ behavior observed for globular clusters within ~ 50 kpc of the center of the cD galaxy NGC 3311 (McLaughlin et al. 1995). In this case, there will be 1.9 times as many globular clusters in our field as in the MHH94 field. Given the magnitude shift and this multiplicative factor we may scale the MHH94 data for M87 globulars to our field. The predicted globular cluster counts are shown as the dotted curve in Figure 5.

The simple scaling of the M87 globular cluster system to NGC 4874 predicts counts of globular clusters to be higher than the number of Coma cluster objects we detect at $M_R > -12$. This is particularly true for $R \approx 23$ ($M_R \approx -12$), where we can tell that most of our objects are resolved, contrary to the prediction of the M87 globular cluster scaling. This is not a worry, because an acceptable range of values for the Coma/Virgo distance ratio, the density gradient of the globular clusters, or the specific frequency of clusters in NGC 4874 could easily accommodate a factor 2 change in the estimated globular cluster

density. What this estimate does show, however, is that it is unlikely that our faintest bins contain predominately dwarf galaxies. Rather the globular clusters are probably a major component of our faintest detections.

We refrain from attempting to constrain the parameters of the NGC 4874 globular cluster population—such as their luminosity function and radial distribution—because our resolution does not permit a satisfactory discrimination against dwarf galaxies. From Figure 5 it should be apparent that any effort to study dwarf galaxies or globular clusters at $M_R \gtrsim -11$ must have sufficient resolution to distinguish the two. At the distance of the Coma cluster, the refurbished HST is an excellent tool for studying the globular clusters (see Baum et al. 1994), since they are unresolved and easily detected, while the dwarf galaxies of $\gtrsim 100$ pc size will be quite well resolved. Indeed because of their low surface brightness and the relatively small and slow optics of the HST, it would take roughly 20 hours of exposure time to detect the dwarfs with the HST.

5.3. Mass Constraints on Dwarf Galaxies

It is apparent from Figure 7 that the total visible luminosity from very faint galaxies $(-9.4 > M_R > -15)$ in the Coma core is at most a few percent of the light emitted by the giant galaxies of the region $(M_R \leq -18)$. We wish to estimate whether the mass in the dE's is also negligible compared to the giants. We can make only the crudest estimates of the mass necessary to keep the dwarf galaxies bound in the face of tidal forces from the cluster potential, because we know little about the detailed shapes of the Coma dwarfs, nor is the cluster potential well known. Assume a dwarf galaxy of mass m and radius r_t to be adrift at distance r from the center of an isothermal potential well with 1-dimensional velocity dispersion σ . Tidal forces will strip stars from the periphery of the dwarf unless

$$\frac{Gm}{r_t^3} \ge \frac{2\sigma^2}{r^2}. (7)$$

None of the quantities r_t , σ , or r is particularly well determined from our data, but we can make some estimates. From Figure 7, we find that the typical R=23 Coma dwarf $(M_R=-12)$ fits an exponential scale length of $r_s=200$ pc. Assume that the galaxy extends for k scale lengths before reaching the truncation radius r_t . If we assume that the Coma dwarfs have King (1966) mass and light profiles with concentration parameters 2 < c < 6, then we find that $k \approx 10$. We have no direct evidence, however, that the Coma dwarfs extend for 10 scale lengths. We conservatively assume that they are truncated at only 3 scale lengths.

The velocity dispersion of the Coma cluster is $\sim 1000~\rm km~s^{-1}$, but the regions close to NGC 4874 might be well inside the core radius of the cluster potential, where the tidal forces can be quite different from the right-hand-side of Equation (7). Instead we will assume the dwarfs to be in an isothermal potential with $\sigma = 250~\rm km~s^{-1}$, which is the measured central dispersion of NGC 4874 (Faber *et al.* 1989). The globular cluster system of M87 has dynamics consistent with such a potential well within 50 kpc radius (Merritt & Tremblay 1993). We observe the projected dwarf galaxy density to be rising at distances $\lesssim 1'$ from NGC 4874, so we assume $r \approx 30h_{75}^{-1}~\rm kpc$. Equation (7) can be rearranged as

$$\left(\frac{m}{L}\right) \ge 2.3h_{75} \left(\frac{m_{\odot}}{L_{\odot}}\right) 10^{0.4(R-23)} \left(\frac{k}{3}\right)^3 \left(\frac{r_s}{200 \,\mathrm{pc}}\right)^3 \left(\frac{\sigma}{250 \,\mathrm{km \, s^{-1}}}\right)^2 \left(\frac{r}{30 \,\mathrm{kpc}}\right)^{-2}, \quad (8)$$

where the luminosities are in R band. The Local Group dwarf spheroidals have m/L in the range 10–100 (FB94 and references therein), and would thus probably survive without serious tidal stripping if dropped into the NGC 4874 potential well. There is no need for the Coma dwarfs to have extraordinary m/L values to be long-lived, and thus they likely contribute negligibly to the total mass of the cluster (assuming that the radial density gradient of the dwarfs is at least as steep as that of the giants throughout the cluster). This conclusion is, however, strongly dependent on the nature of the gravitational potential and tidal field in the inner 100 kpc of the cluster. The mass distribution in this region is quite uncertain, so these conclusions could easily require revision.

Note that the m/L value required to maintain integrity in the tidal field scales as r_s^3/L . At a given magnitude, tidal destruction could produce an upper limit to the r_s (or equivalently a lower μ_0 limit) distribution of dwarfs in Coma.

Dwarf galaxies in the Coma core are heated by encounters with giant galaxies due to tidal forces. The dwarf galaxies could become unbound if enough energy is injected over the ~ 5 Gyr since the creation of the Coma cluster. We calculate that the m/L ratios necessary to stave off this effect are an order of magnitude lower than the estimate in Equation (8), and can be safely ignored.

6. Implications and Conclusions

We have measured the LF in the Coma cluster core to fainter absolute magnitudes $(M_R=-11.4,\,L=2h_{75}^{-2}\times 10^6L_{\odot})$ than any other LF study of which we are aware, and with a broader sensitivity in surface brightness (the recent De Propris *et al.* [1995] study is

to similar depth as ours). We have found that an $\alpha = -1.4$ power law describes the LF down to luminosities typical of the Local Group dwarf spheroidal galaxies. These most extreme Coma cluster galaxies have sizes comparable to Local Group galaxies at a given absolute magnitude. This should be a useful constraint for theories of galaxy formation. We have, however, performed this measurement in a most extreme environment, one of the densest regions of the nearby Universe—there are 10⁵–10⁶ galaxies per Mpc³ in the Coma core, compared to 10-100 per Mpc³ in the Local Group. This complicates comparison to the general field LF because of the many additional processes which could have influenced the development of the Coma dwarfs, such as the increased pressure and tides in the cluster environment. The significance of these results to theories of galaxy or cluster formation depends upon the evolutionary history of the Coma dwarfs: are their formation and evolution identical to those of field dwarfs, merely being concentrated for our convenience in the core of the cluster? Or, at the other extreme, are they formed by processes that exist solely in the cluster core, giving them little relation to faint Local Group or field galaxies? We first discuss the possibility that Coma and field dwarfs are very similar, and then move on to scenarios for the Coma dwarfs that are increasingly disparate from those of field galaxies. We refer the reader also to the FB94 review for discussions of evolutionary scenarios for dE galaxies; the formation of dwarf galaxies (indeed all galaxies) is poorly understood—it is not even clear what are the dominant physical processes—so we will not go into depth on any particular hypothesis.

6.1. Coma Dwarf Population Similar to the Field Population?

A pleasingly simple interpretation would be that the dwarf galaxies in the Coma cluster core are an entombed, concentrated sample of field dwarf galaxies. The giant galaxies in the Coma cluster are extremely atypical compared to the field, being nearly completely devoid of late types. Dwarf galaxies, however, are much less massive and thus less subject to dynamical friction than giants. Furthermore they are smaller, and could (depending on the scaling of m/r_t^3 with L) be less subject to tidal disruption than the giants, with our simplest calculations indicating that Local Group dwarfs would not be severely harmed by the tidal field around NGC 4874. Thus a dwarf galaxy probably has a better chance than a giant of inhabiting the cluster environment without substantial merging or destruction. It is likely, however, that dwarf galaxies in the Coma cluster would be stripped of gas (FB94), and thus the episodic star formation history that seems characteristic of the Local Group dwarfs (see FB94 for review) would have been truncated for the Coma dwarfs soon after the development of the hot intra-cluster medium. This of course has been advanced as an

explanation of the apparent deficit of dwarf irregular galaxies in clusters relative to the field, as discussed by FB94. They also note, however, the dominance of gas-stripped dE's over gas-rich irregular dwarfs in regions of Virgo where stripping should *not* be important, indicting some internal mechanism as the agent of gas stripping, rather than ram pressure. Thus it is possible that the Coma cluster medium has had little evolutionary effect on the dwarfs we observe to be resident there.

In this most simplistic case, the Coma dwarfs are a typical population of low-luminosity galaxies, save that they have had no recent star formation episodes to significantly perturb their luminosities. The agreement between our faint-end LF slope and those from the Virgo studies (SBT85 and the LSB extension of Impey, Bothun, & Malin 1988) supports the idea of a universal mass function (or more precisely, universal stellar mass function) for dwarf galaxies. Of course should the much steeper cluster LF slopes measured by De Propris et al. (1995) be confirmed, we would have to abandon this point of view.

The main problem with the idea of a universal faint-end LF is that field surveys yield shallower slopes: $\alpha = -0.97 \pm 0.25$ from Loveday et al. (1992); $\alpha = -1.0 \pm 0.2$ from Marzke, Huchra, & Geller (1994); $\alpha = -1.1$ from Ellis et al. (1995). In the Local Group the LF may be determined for even fainter galaxies than in our study: van den Bergh (1992) fits $\alpha = -1.1$ to the Local Group galaxy LF for $M_V < -7.6$. With new Local Group dwarfs being discovered on an annual basis, however, it is possible that this slope will steepen with time. Babul & Rees (1992) proposed that dwarf galaxies are born with common mass functions in both cluster and field environments. Field dwarfs might effectively blow themselves up in star formation incidents, but cluster dwarfs would remain confined by the pressure of the intra-cluster medium. In this view the field LF vs. cluster LF dichotomy is real and due to the demise of field dwarfs. We have found a faint-end LF in Coma similar to that in Virgo, and Thompson & Gregory (1993) also report a dwarf-to-giant ratio similar in Coma and Virgo, despite the former being a denser environment. Thus if the Babul & Rees scenario is correct, then the confinement effect may "saturate" at Virgo densities—the additional pressure in Coma preserves no more dwarfs, and $\alpha \approx -1.4$ represents the "intrinsic" dE LF. Countering this view somewhat is the observation that Coma cluster dwarf galaxies have similar sizes—and perhaps similar masses—to the Local Group dwarfs at comparable magnitudes. If dE evolution is strongly controlled by local pressure, would we expect Local Group and Coma cluster objects to be this similar?

Another school of thought on the field/cluster LF dichotomy is that the differences are primarily due to selection effects. In particular, it is suggested that cluster LF studies are generally done with deeper images than are nearby field surveys, resulting in omission of LSB galaxies from the field surveys. The field survey of Ellis *et al.* (1995), for example,

selects target galaxies from a survey with limiting surface brightness 26.5 b_J mag arcsec⁻², substantially shallower than the Virgo, Fornax, and Coma cluster surveys discussed here. Deep field redshift surveys seem to show an increase in the LF slope at higher redshifts (Ellis et al. 1995; Eales 1993), which could likewise be due to the fact that deep redshift survey targets are selected from deeper photographic or CCD exposures with more sensitivity to LSB objects. Some steepening in the LF even at fixed SB sensitivity does, however, seem to be indicated by the Ellis et al. (1995) survey, since their $z \approx 0$ and their $z \approx 0.3$ LFs are constructed from the same parent survey, with a single SB threshold, yet they find a steeper LF at higher z. Ferguson & McGaugh (1995) also suggest that local field LF slopes are depressed by failure to count LSB galaxies. This may be evidenced by the excess (over the $\alpha = -1.0$ prediction) of nearby $-16 < M_{\rm Zw} < -13$ galaxies seen in the CfA survey by Marzke, Huchra, & Geller (1994). Marzke et al. (1994) attribute this excess to a population of Sm-Im galaxies with $\alpha = -1.87$; the relation of such galaxies to cluster dE's is unclear. Sprayberry et al. (1995) report observations of the field LF that have the faint-end slope significantly increased when they make extra effort to reduce surface-brightness biases.

Gronwall & Koo (1995) derive a z=0 field LF for galaxies by requiring a best fit to faint galaxy count, color, and redshift survey data. They claim that most of these data can be explained by allowing the local LF to steepen to $\alpha \approx -1.5$ at $M_{B_J} > -17$, where local information is sparse. Such behavior would be consistent also with our Coma cluster LF. Their derived LF is consistent with the Loveday *et al.* (1992) LF, but may disagree with the deeper Ellis *et al.* (1995) $M_{B_J} < -15$ LF.

Should the field LFs somehow be reconciled with the Coma or Virgo LFs, or the Gronwall & Koo LF, we would be led to suspect some internal process (e.g. supernova heating) as the driver of dwarf galaxy evolution rather than environmental variables such as pressure or ionizing radiation field.

6.2. Inhibition or Destruction of Cluster Dwarfs

While the Babul & Rees (1992) scenario invokes the intra-cluster medium to *increase* the number of dwarfs in clusters over the field counts, there are of course processes that could *reduce* the number of cluster dwarfs, especially within 100 kpc of the Coma cluster core. While our simple calculations suggested that tidal forces are not important, a more interesting test will be to compare the size distributions of the Coma dwarfs to those in the Virgo cluster. In a further publication, after re-analyzing the most diffuse objects in our image, we will compare the maximum sizes of galaxies in the Coma core to those found in

Virgo. Should the latter be larger at a given magnitude, it would suggest tidal forces are indeed at work in Coma. For now we simply note that the $M_R \approx -12$ galaxies in the Coma cluster do not appear to be depleted near the core, as might be expected were tidal forces destroying most dwarfs.

6.3. Satellites of NGC 4874

The dwarf galaxies in our image show a strong concentration toward the giant elliptical NGC 4874, which may not be the dynamical center of the Coma cluster. It may be incorrect to think of these dwarfs as belonging to the cluster; a more appropriate description may be as satellites of NGC 4874. The spatial distribution of dwarfs around NGC 4874 is consistent with that observed for satellites of field ellipticals (Vader & Sandage 1991) and of field spirals (Zaritsky et al. 1993), albeit far richer. The neighborhoods of giant ellipticals may be particularly fertile for production of dwarf galaxies. It would be interesting to see whether NGC 4889, or NGC 4881, which are giant Coma cluster ellipticals with apparently lower specific frequencies of globular clusters than NGC 4874 (Harris 1987; Baum et al. 1995), also have fewer dwarf galaxies in their vicinities. Note in Figure 8, however, that the brightest galaxies in Coma may have an equally strong concentration toward NGC 4874, though the number of objects in the nearest bin is small (5). Note further that we did not detect any concentration of dwarf galaxies around the other elliptical galaxies in our Coma field—but these are each at least ten times less luminous than NGC 4874. If the dwarf galaxies which we have detected in the Coma core are members of an enhanced satellite population, then the comparison to the field LF is further complicated, and environmental mechanisms are of course implicated in the formation and evolution of these galaxies.

In this context it is worth noting that the diffuse light, globular cluster density, and dwarf galaxy density seem to have similar radial structure on the outskirts of NGC 4874. McLaughlin et al. (1995) note that all the current data on globular cluster populations around giant ellipticals are consistent with the idea that globular clusters and cD envelopes (as opposed to the "bodies" of cD galaxies, which follow an $r^{-1/4}$ profile) always have common structure. NGC 4874 is classified as a cD galaxy by Schombert (1988), and our data are taken at large enough distances from its center that the envelope light is dominant, by his definitions. If the globular clusters are part of the same system as the diffuse envelope, then our data may be suggesting that the formation of the dwarf galaxies is likewise integrally connected with the mysterious origin of the cD envelope.

6.4. Dwarfs as Shards

In the above subsections we assumed that the objects we detect in a cloud around NGC 4874 are long-lived and predate the cluster. Neither need be true—the dwarfs could be pieces of larger galaxies destroyed by the cluster tidal fields or through interaction with NGC 4874. They could also be in the process of dissolution. Note that the dwarf galaxies show roughly the same spatial distribution as the diffuse flux around NGC 4874, but with only a few percent as much total luminosity. If dwarf "galaxies" are constantly being formed and dissolved near NGC 4874, then each must typically live at least a few percent of the age of the system, else there will be too much diffuse light left over. We would perhaps expect, however, to see large numbers of very extended dwarfs were there a continual process of dissolution, and we do not. If the stellar contents of the dwarfs were to fade before becoming part of the diffuse light, then the dwarfs could be even shorter-lived, and we might not detect them in their most diffuse state. Color or spectral information would fairly quickly tell us whether in fact these objects are transient ($\leq 10^7$ year) starburst phenomena.

The similarity between the diffuse light and the dwarf galaxy gradient suggests a common, unknown origin. It is often suggested that cD galaxy halos are the remains of galactic cannibalism. If the dwarf galaxies are shards of NGC 4874's victims, then their colors should resemble those of the old populations of giant galaxies. The colors of field and cluster dE's more closely resemble those of metal-poor globular clusters.

A further point worth noting about the diffuse light is that it is, in a nutshell, diffuse. We calculate that the visible (R) component of the hot intracluster bremsstrahlung radiation [detected in X-rays, cf. White, Briel, & Henry (1993)] is several orders of magnitude weaker than the detected R-band flux, so that most of the R-band should be starlight. Our sensitivity is such that any unresolved clumps brighter than $M_R = -9.4$, or $3 \times 10^5 L_{\odot}$, would be detected. Yet the total flux in such lumps is still only a few percent of the diffuse flux. Even if we were to extrapolate the $\alpha = -1.4$ LF to zero-luminosity galaxies, we would not have enough flux to make up the diffuse light. If the diffuse light is lumpy, the lumps must be quite small. Scheick & Kuhn (1994) similarly conclude, from a search for surface-brightness fluctuations in the diffuse light of the cluster Abell 2670, that the typical unit of luminosity in the diffuse light must be $\leq 3 \times 10^3 L_{\odot}$. Thus if the diffuse light is formed from disrupted galaxies, the remnants are very effectively dispersed It would seem odd for $10^6 L_{\odot}$ objects to be left behind, with scale sizes of ~ 200 pc just like Local Group dSph's. The origin of the cloud of diffuse light, globular clusters, and dwarf galaxies surrounding NGC 4874 begs further investigation, especially since the flux of starlight in the diffuse component is comparable to the total amount in galaxies of any

size within the central 100 kpc.

6.5. Implications for the Coma Cluster

Finally, the observations presented in this paper have implications for the Coma cluster as a whole. As stated earlier, the implied total amount of mass in previously undetected galaxies and globular clusters is insignificant compared to that already postulated from the brighter galaxies in the cluster (assuming mass-to-light ratios consistent with those measured in the Local Group dwarfs). The Coma dwarfs would need to have mass-to-light ratios several orders of magnitude greater than any previously measured dwarf galaxy to have a significant impact on the total mass of the cluster. We have surveyed and catalogued all objects in the center of Coma having luminosities of globular clusters or brighter, plus we have measured the diffuse halo light. It is thus highly unlikely that there remains undetected, visibly luminous matter sufficient to close the cluster. White et al. (1993) have carried out a full inventory of the x-ray gas mass in Coma and also find this to be grossly insufficient to close the cluster. Unless there is a large population of extremely faint massive objects in Coma, we are left once again with the hypothesis that Coma and clusters in general are dominated by non-luminous mass. Recent observations of microlensing by massive compact objects in our own galaxy suggest that only $\sim 20\%$ of the total galaxy mass can be accounted for in extremely faint baryonic objects (Gates et al. 1995). Thus, even if every one of the Coma galaxies had a population of MACHOS, it would not close the cluster. These circumstances continue to suggest the presence of non-baryonic dark matter in the cluster.

The discussion above also has bearing on recent claims of a baryon crisis in Coma. White et al. (1993) have suggested that the amount of baryons seen in Coma is in conflict with the bounds set from nucleosynthesis. Our observations have shown that the amount of baryons in faint, previously unknown objects is inconsequential to this argument. The extra amount of baryonic mass added to their inventory of the cluster is well within their quoted error estimates.

7. Summary and Future Directions

Our census of the population of galaxies in the Coma cluster has produced a few basic facts about extremely faint galaxies: first, the LF in the extraordinarily dense Coma cluster core is similar in shape to that measured in the Virgo cluster by SBT85, though our survey extends to fainter magnitudes, and is sensitive to both higher and lower surface brightness dwarf galaxies. A power law with $\alpha=-1.4$ describes both populations fairly well, down to $M_R=-11.4$ in our study. Further extrapolation of this law to $M_R=-9.4$ is consistent with our data and those of TV87, in the regime where globular clusters are easily confused with dwarf galaxies. This LF is in conflict with field LF studies and the LF of known Local Group members, both of which seem to indicate shallower faint-end slopes. On the other hand, the sizes and masses of the faintest detected Coma galaxies seem roughly consistent with those of Local Group dwarf galaxies of similar luminosity, and there is as yet little evidence that the Coma dwarfs have had their evolution severely affected by their proximity to NGC 4874. The $M_R \sim -12$ dwarf galaxies follow the diffuse light and globular cluster populations in a strong concentration near NGC 4874, with all three increasing in density as $r^{-1.3}$ towards this cD galaxy. This gradient is similar to that observed for globular clusters and dwarf galaxies around giant ellipticals in the field, so it may be that we are viewing a population that was born with NGC 4874.

The collection of these data is not a severe challenge for modern instrumentation, and extension of this work would be straightforward. Indeed further such observations of Coma and other distant clusters are in progress (e.g. Secker & Harris 1994; De Propris et al. 1995). Our caution to future investigators is that the quality of background correction is both improved and more easily assessed if control fields covering several times the area of the target fields are obtained. Many newer telescopes routinely obtain seeing of 0.8" or better; in such conditions, the distinction between galaxies and globular clusters would be easier, and the Coma galaxy LF could be extended another magnitude or so fainter. HST images could be used to identify the globular clusters and remove them from the galaxy LF (HST images of control fields would be necessary as well).

Are the Coma cluster dwarfs similar to Local Group or field dE's? A measure of the colors of the Coma dwarfs is clearly called for. Do they match those of field, Local Group, or Virgo dwarfs? Is there any sign of recent star formation in these objects? This seems unlikely, but color information could rule out any sort of transient nature for these structures. Colors as blue as the Virgo dE's (Caldwell & Bothun 1987) would rule out an origin as remnants of destroyed larger galaxies. In measuring these colors, extensive color information on control fields would of course have to be obtained, since the background subtraction techniques we have employed would have to be implemented on the color-magnitude plane.

Spectroscopic information will be difficult to obtain given the faint apparent magnitudes, but a measure of the velocities of these many dwarfs could enlighten us as to the dynamical state of the inner regions of Coma, where there are not enough giants to learn about the dynamics. Of course spectral information would also tell us about the stellar populations and metal content of these dwarfs.

The Coma cluster is useful in that it contains two cD galaxies and a third giant elliptical (Schombert 1988). Replicating our study near NGC 4889 and NGC 4881 would enlighten us as to whether the dwarfs are truly associated with the bottom of the cluster potential well, or whether they are found in large numbers in the vicinity of all giant ellipticals, or only near cD galaxies. Invaluable clues to their origin would result. It may be difficult to search for the $M_R \sim -12$ galaxies on the outskirts of Coma, as their numbers may become too sparse to detect in the midst of background galaxy density fluctuations.

We thus hope that our Coma census will be a cornerstone for these future studies, which will build up the edifice of dwarf galaxy formation theory. Thousands of these galaxies are accessible to observations by modern instrumentation, which will help determine the extent to which cluster dE's and field dwarf galaxies share a common structure or history.

Thanks to P. Teague for assistance in the Coma observing run, and to P. Guhathakurta for allowing us to commandeer images from other projects for use as control fields. We thank N. Metcalfe for providing an electronic version of the GMP83 galaxy catalog. GMB was generously supported by AT&T Bell Laboratories and the Bok Fellowship from Steward Observatory during the tortuously extended duration of this work. GMB also thanks E. Olszewski, N. Caldwell, C. Impey, and M. Mateo for discussions of dwarf galaxies. MPU thanks A. Sandage for discussions at the inception of this project, and Northwestern University and NASA for partial support.

REFERENCES

Babul, A. & Rees, M. 1992, MNRAS, 255, 346

Baum, W. A. et al. 1994, BAAS, 26, 1398

Biviano, A. et al. 1995, A&A (submitted)

Bothun, G. D., Impey, C. D., & Malin, D. F. 1991, ApJ, 376, 404.

Burstein & Heiles 1982, AJ, 87, 1165

Caldwell, N., Armandroff, T. E., Seitzer, P., & Da Costa, G. S. 1992, AJ, 103, 840

Caldwell, N., & Bothun, G. D. 1987, AJ, 94, 1126

De Propris, R., Pritchet, C. J., Harris, W. E., & McClure, R. D. 1995, ApJ (in press)

de Vaucouleurs, G., et al. 1991, Third Reference Catalogue of Bright Galaxies, Springer-Verlag, New York

Disney, M. 1973, ApJ, 181, L55

Driver, S. P., Phillipps, S., Davies, J. I., Morgan, I., & Disney, M. J. 1994, MNRAS, 268, 393

Dow, K. L., & White, S. D. M. 1995, ApJ, 439, 113

Eales, S. J. 1993, ApJ, 404, 51.

Ellis, R.S., Colless, M., Broadhurst, T.J., Heyl, J.S. & Glazebrook, K. 1995 (in preparation)

Faber, S. M. et al. 1989, ApJS, 69, 763.

Ferguson, H. C. 1993, MNRAS, 263, 343

Feguson, H. C. & Binggeli, B. 1994, A&ARev, 6, 67 (FB94)

Ferguson, H. C., & McGaugh, S. S. 1995, ApJ, 440, 470

Ferguson, H. C., & Sandage, A. 1988, AJ, 96, 1520 (FS88)

Ferguson, H. C., & Sandage, A. 1991, AJ, 101, 765

Gates, E. I., Gyuk, G., & Turner, M. S. 1995, Phys.Rev.Lett, (submitted)

Godwin, Metcalfe, & Peach 1983, MNRAS, 202, 113 (GMP83)

Gronwall, C., & Koo, D. C. 1995, ApJ, 440, L1

Harris, W. E. 1987, ApJ, 315, L29

Hopp, U., Wagner, S. J., & Richtler, T. 1995, A&A (in press)

Impey, C., Bothun, G., & Malin, D. 1988, ApJ, 330, 634

King, I. R. 1966, AJ, 71, 64

King, I. R. 1971, PASP, 83, 199

Loveday, J., Peterson, B. A., Efstathiou, G., & Maddox, S. J. 1992, ApJ, 390, 338

Lugger, P. M. 1986, ApJ, 303, 535

Marzke, R. O., Huchra, J. P., & Geller, M. J. 1994, ApJ, 428, 43.

Mazure, A., Proust, D., Mathez, G., & Mellier, Y. 1988, A&AS, 76, 339

McLaughlin, D. E., Harris, W. E., & Hanes, D. A. 1994, ApJ, 422, 486 (MHH94)

McLaughlin, D. E., Secker, J., Harris, W. E., & Geisler, D. 1995, AJ, 109, 1033

Merritt, D., & Tremblay, B. 1993, AJ, 106, 2229

Ratnatunga, K. 1993 (private communication).

Reed, B. C., Hesser, H. E., & Shawl, S. J. 1988, PASP, 100, 545

Romani, R. W. & Maoz, D. (1992), ApJ, 386, 36

Sandage, A., Binggeli, B., & Tammann, G. A. 1985, AJ, 90, 1759. (SBT85)

Schombert, J. M. 1988, ApJ, 328, 475

Secker, J. & Harris, W. E. 1994, BAAS, 26, 1497

Sprayberry, D., Impey, C., Irwin, M., & Bothun, G. 1995 (in preparation).

Thompson, L. A., & Gregory, S. A. 1993, AJ, 106, 2197

Thompson, L. A. & Valdes, F. 1987, ApJ, 315, L35 (TV87)

Turner, J. A., Phillipps, S., Davies, J. I., & Disney, M. J. 1993, MNRAS, 261, 39

Tyson, J. A. 1986, J. Opt. Soc. Am. A, 3, 2131

Tyson, J. A. 1988, AJ, 96, 1

Tyson, J. A. & Seitzer, P. 1988, ApJ, 335, 552 (TS88)

Ulmer, M. P., Wirth, G. D., & Kowalski, M. P. 1992, ApJ, 397, 430

Ulmer, M. P., Nichol, R. C., Bernstein, G. M., & Tyson, J. A. 1995 (in preparation)

van den Bergh, S., 1992, A&A, 264, 75.

Vader, J. P., & Sandage, A. 1991, ApJ, 379, L1

Valdes, F. 1989, in Proc. 1st ESO/ST-ECF Data Analysis Workshop, edited by P. J. Grosbol, F. Murtagh, & R. H. Warmels (ESO: Garching)

White, S.D.M., Briel, U. G., and J. P. Henry, 1993, MNRAS, 261, L8

White, S. D. M., Navarro, J. F., Evrard, A. E., & Frenk, C. S. 1993, Nature, 366, 429

Zaritsky, D, Smith, R., Frenk, C., & White, S. D. M. 1993, ApJ, 405, 464

This preprint was prepared with the AAS IATEX macros v3.0.

Figure Captions

- Fig. 1.— Deep CCD Image of the Coma Core. This image is approximately 7.5′ square; North is up, East is to the left, and the intensity has been logarithmically scaled to increase the dynamic range. NGC 4874 is just off the N edge at the right half of the image; the diffuse light gradient from NGC 4874 is evident across the entire field.
- Fig. 2.— Cleaned Image of the Coma Core. The same CCD field as shown in Figure 1 is shown here after subtraction of the diffuse light signal and the elliptical models of the brightest objects. Areas with large residuals to these models are masked off. This image is linearly scaled, and thousands of faint objects are now visible, with a marked gradient toward NGC 4874.
- Fig. 3.— Magnitude-Resolution Distribution of Coma Field. Resolution parameter \mathcal{R} and total magnitude in the R band are shown for all objects in the Coma field catalog. Objects in the region with R < 21 and $\mathcal{R} < 0.8$ are assumed to be foreground stars since they are unresolved and distinct from the galaxy population.

Fig. 4.— Object Counts and Completeness. The upper plot shows the detection efficiency for unresolved objects as a function of magnitude, as derived from the Monte Carlo tests described in §2.7. The heavy solid line is for the Coma field, while the five dotted lines are for the five control fields. The lower panel shows the number of objects detected per magnitude for the Coma field as the histogram; stars are excluded from the counts for R < 21. The triangles with error bars give the estimated background counts \tilde{N}_{bg} and the uncertainties σ_{bg} derived from the control fields. The dashed line shows the $dN/dm \propto \text{dex}(-0.39R)$ power-law behavior expected of the background counts (Tyson 1988), and the dotted line shows the star counts expected in the model of Ratnatunga (1993).

Fig. 5.— Luminosity Function of the Coma Cluster Core. The filled circles show the number N_{cl} of objects present in the Coma cluster core within the area of our CCD image. The open triangles are our best estimate of the number of resolved objects in these bins; in brighter bins, essentially all objects are resolved, and unresolved in fainter bins. The open circles show the number of objects per magnitude within 8' of NGC 4874 from the GMP83 photographic catalog. All points have also been corrected for background counts and incompleteness, and scaled to the 52.2 arcmin² area of the CCD field. The straight line is the best fit power-law to the luminosity function over the range 15.5 < R < 23.5. This best fit has $dN/dL \propto L^{\alpha}$ with $\alpha = -1.42 \pm 0.05$. If the measured globular cluster population around M87 were moved to NGC 4874 as described in §5.2., we would have detected the number of globular clusters shown by the dotted line. Thus it is likely that the majority of the R > 23.5 objects in the cluster are globular clusters rather than galaxies. The absolute magnitude scale on top assumes a distance modulus of 34.9 to the Coma cluster.

Fig. 6.— Resolution Distribution of Coma Cluster Members. The histogram in each panel shows, for the indicated magnitude range, the number of objects in the Coma field as a function of measured resolution parameter. The background contribution in each bin has been estimated from the control fields and subtracted; the error bars show the uncertainty due to background count fluctuations. The dotted curves show the distributions of resolution parameter expected from a population of unresolved objects. For the brightest two bins shown here there must be a sizable contribution from resolved objects, whereas the fainter 4 bins are consistent with the unresolved distribution.

Fig. 7.— Sizes of Faint Coma Members. This plot shows the distribution of magnitude and exponential scale length for the very faint objects we detect in the Coma cluster core. The heavily shaded region shows the typical sizes of Coma cluster galaxies with 22.5 < R < 23.25. There are relatively few Coma galaxies in this magnitude range with scale lengths above or below the shaded range. For R > 23.25, our ability to determine the sizes of the population is diminished, but we detect many objects. The lightly hatched region outlines the ranges of galaxy magnitude and size which these objects could have. The heavy line at right is the locus of 50% detection efficiency; we are seriously incomplete to the right of this line. The Local Group dwarf spheroidal galaxies (save Fornax, which is too bright) are labelled at their respective locations in this magnitude, size plane. The sizes of the extremely faint Coma cluster galaxies seem to be similar to the sizes of Local Group galaxies at comparable luminosity. Our sensitivity is sufficient to detect most of the Local Group dSph's at the distance of the Coma cluster.

Fig. 8.— Radial Distributions of Coma Cluster Members. The mean R surface brightness contributed by Coma cluster members of various magnitudes is shown as a function of distance r from NGC 4874. The legend lists the magnitude ranges corresponding to the various symbols; in all cases, the error bars reflect uncertainties in the background levels, as described in the text. The dotted lines trace a surface brightness dropping as $r^{-1.3}$. The diffuse light and all of the discrete objects are consistent with this radial dependence, except that galaxies of moderate brightness ($-17.4 < M_b < -14.9$, filled triangles) seem to flatten for $r \lesssim 5'$. Somewhat fainter galaxies ($-14.4 < M_R < -12.4$, squares) may also have a central deficit, but the bright galaxies, extremely faint galaxies ($M_R > -12.4$), and globular clusters are consistent with the power law across the sampled range in r. The total light contributed by very faint galaxies is small compared to the surface brightness in diffuse light or in galaxies at the brightest bin. The brightness of the night sky in R band is 20.3 mag arcsec⁻².

Table 1. Fields Observed

Name	RA Dec. (1950)		l	b	Area (arcmin²)	FWHM ^a (arcsec)	Noise Density ^a $(R \text{ mag arcsec}^{-1})$	A_R (mag)
Coma	12 ^h 57 ^m 17 ^s	+28°09′35″	56°	$+88^{\circ}$ -46° -43°	52.2	1.31	28.07	0.00
SA68	00 ^h 14 ^m 53 ^s	+15°29′27″	111°		54.2	1.31	27.94	0.02
0427	04 ^h 27 ^m 56 ^s	-36°24′09″	238°		52.9	1.30	28.02	0.00
0909	09 ^h 09 ^m 57 ^s	-07°38′18″	238°	$+26^{\circ} +45^{\circ} +35^{\circ}$	53.9	1.28	28.09	0.06
Ser1	15 ^h 13 ^m 13 ^s	+00°49′46″	0°		54.1	1.33	27.98	0.12
Her1	17 ^h 20 ^m 39 ^s	+50°06′19″	76°		54.7	1.32	28.12	0.01

 $^{^{\}rm a}{\rm After}$ degradation to match Coma.

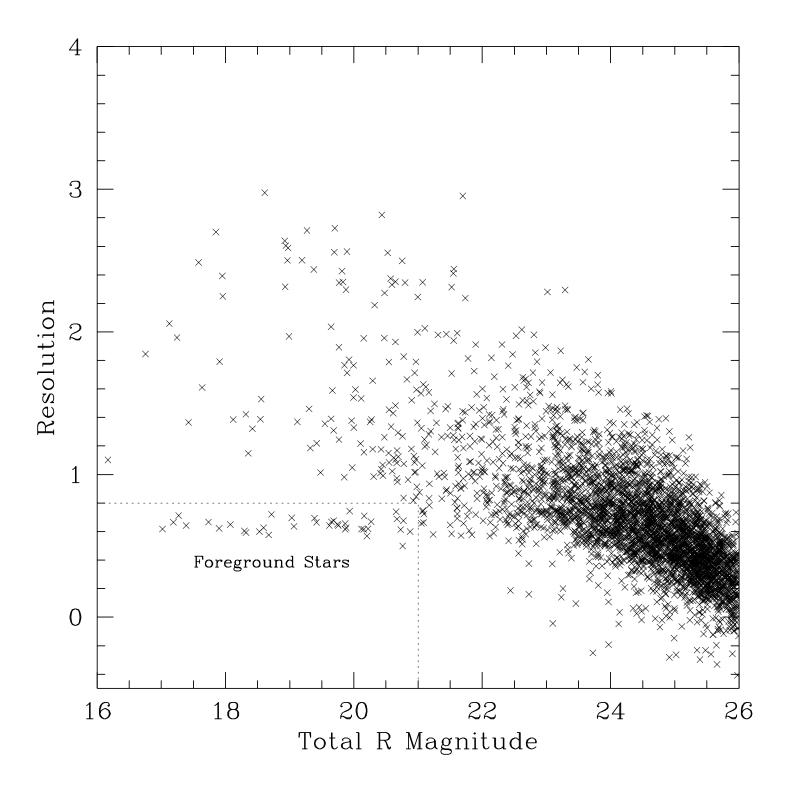
Table 2. Coma CCD Object Counts

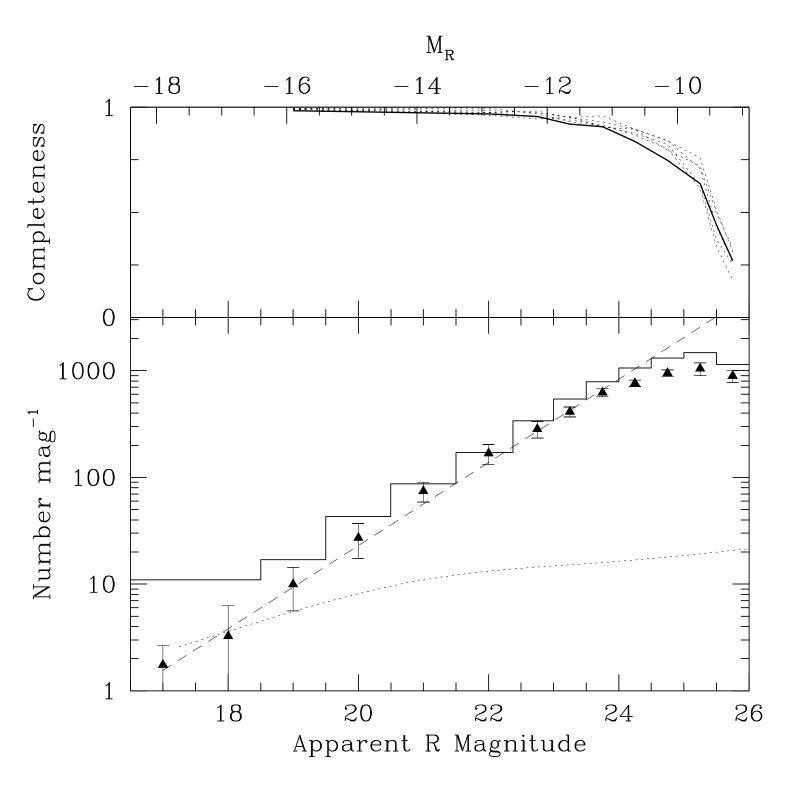
R	N_C	$ ilde{N}_{bg}$	N_{det}	σ_{det}	N_{cl}	σ_{cl}	dN_{cl}/dm	dN_{res}/dm
15.50-16.50	7	0.00	7.00	0.00	7.0	2.6	$7.0 \pm \ 2.6$	
16.50 - 17.50	11	1.75	9.25	0.90	9.2	3.2	$9.2 \pm \ 3.2$	
17.50 - 18.50	11	3.27	7.73	3.01	7.7	4.1	7.7 ± 4.1	
18.50 - 19.50	17	9.96	7.04	4.35	7.2	5.2	7.2 ± 5.2	
19.50 – 20.50	43	27.18	15.82	9.76	16.2	10.8	16.2 ± 10.8	
20.50 – 21.50	87	74.29	12.71	15.50	13.1	16.4	13.1 ± 16.4	27 ± 8
21.50 – 22.50	171	168.34	2.66	35.81	2.1	37.0	2.8 ± 37.0	23 ± 15
22.50 – 23.00	170	142.22	27.78	25.43	29.1	27.2	58.1 ± 54.3	69 ± 16
23.00 – 23.50	272	206.18	65.82	22.19	71.5	25.7	143.1 ± 51.4	100 ± 28
23.50 - 24.00	395	311.33	83.67	26.61	92.2	31.0	184.3 ± 62.0	88 ± 88
24.00 – 24.50	532	381.58	150.42	27.52	179.5	35.9	359.0 ± 71.9	
24.50 – 25.00	658	476.78	181.22	32.34	242.3	46.8	484.6 ± 93.7	
25.00 – 25.50	739	522.40	216.60	71.72	340.6	115.1	$681.\pm 230.$	
25.50 - 26.00	574	446.63	127.37	57.63	471.7	217.5	$943.\pm 435.$	• • •

Table 3. Coma Photographic Object Counts

R	$dN_{cl}/dm^{ m a}$
10–11	0.24 ± 0.24
11–12	0.24 ± 0.24
12-13	-0.03 ± 0.24
13-14	1.85 ± 0.68
14 - 15	3.89 ± 0.99
15 - 16	3.60 ± 0.96
16-17	4.83 ± 1.15
17–18	8.05 ± 1.57

^aObject counts within 8′ of NGC 4874 have been corrected for background and scaled to the area of the CCD field.





Absolute R Magnitude

